Advanced controls and Machine Learning for accelerators

Alexander Scheinker
(ascheink@lanl.gov)

Matter and Technologies 2018

Los Alamos
NATIONAL LABORATORY
EST. 1943


~ 3300 meters
~ 2300 meters


CIC-9: RN91-240-309

Goal: 6D (x,x′,y,y′,z,E) phase space control of particle accelerator beams.

Requirements: Novel non-invasive diagnostics and new adaptive machine learning / feedback control algorithms enabled by these diagnostics.

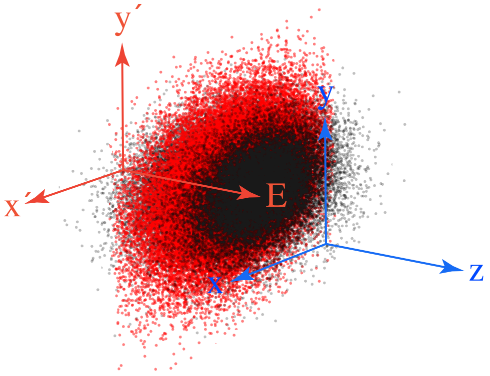

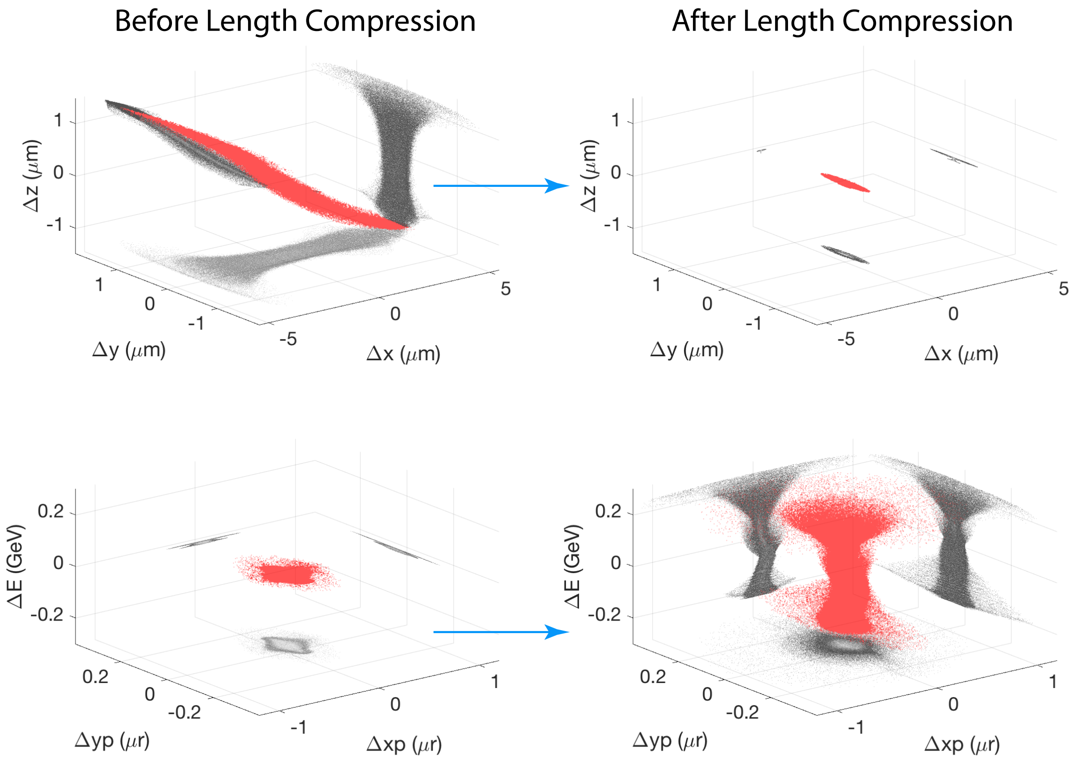

Artificial Intelligence: Machines Tuning Themselves

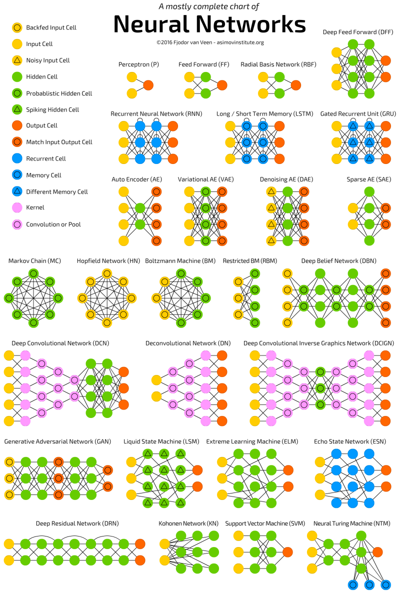

Surrogate models
Big data
Global tuning
Anomaly detection

Ocelot optimization and tuning framework (DESY and LCLS)

Adapative Feedback

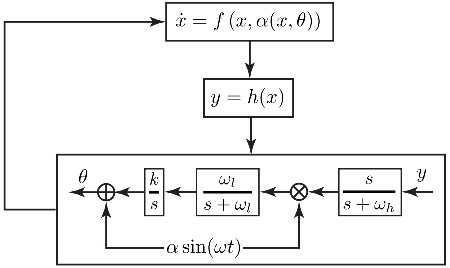

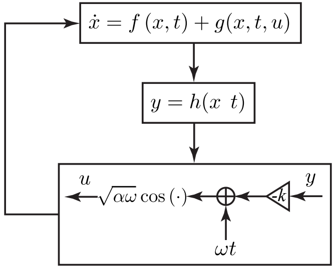

Virtual diagnostics
Real time feedback
Optimization
Phase space tuning

Motivation

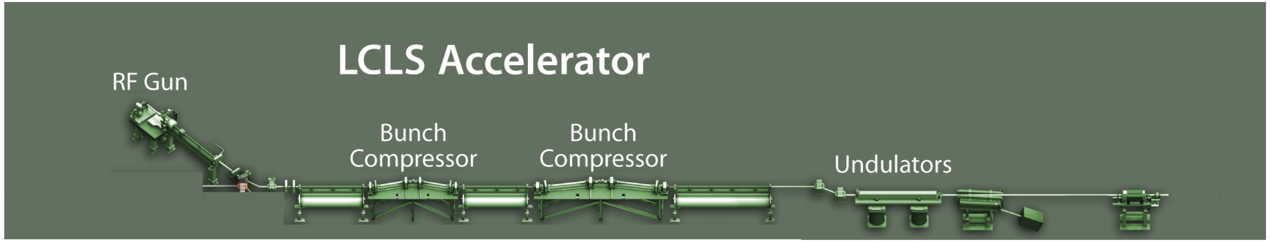
LCLS Accelerator
RF Gun
Bunch Compressor
Bunch Compressor
Undulators

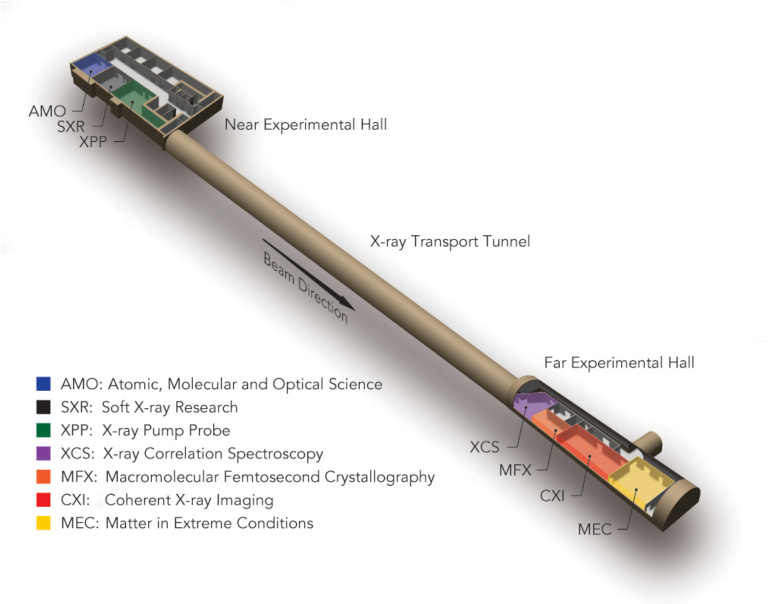
AMO
SXR
XPP
Near Experimental Hall
X-ray Transport Tunnel
Beam Direction
Far Experimental Hall
XCS
MFX
CXI
MEC
AMO: Atomic, Molecular and Optical Science
SXR: Soft X-ray Research
XPP: X-ray Pump Probe
XCS: X-ray Correlation Spectroscopy
MFX: Macromolecular Femtosecond Crystallography
CXI: Coherent X-ray Imaging
MEC: Matter in Extreme Conditions

AMO

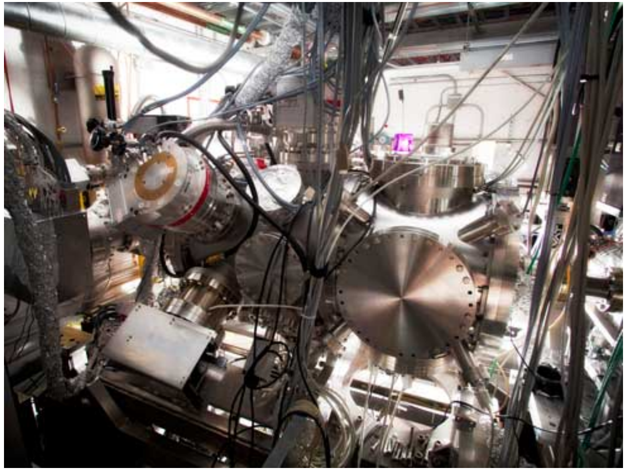

Atomic, Molecular & Optical Science

Soft X-rays for intense ultra short pulses.
Gaseous targets of atoms, molecules, and nanoscale objects: protein crystals or viruses.

Photon energy: 0.48 – 2 keV
Pulse duration: 35 – 300 fs
Low charge mode pulse duration: No
Pulse energy: 1 – 20 mJ @ 266 - 800 nm

Max energy adjustment factor: 4.2
Low charge mode: No

AMO

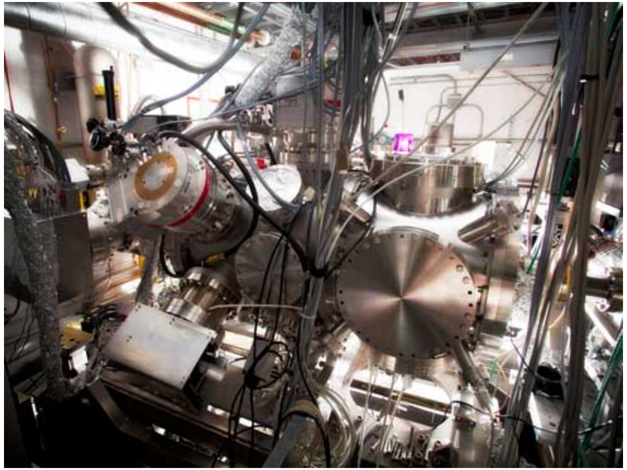

Atomic, Molecular & Optical Science

Soft X-rays for intense ultra short pulses. Gaseous targets of atoms, molecules, and nanoscale objects: protein crystals or viruses.

Photon energy: 0.48 – 2 keV
Pulse duration: 35 – 300 fs
Low charge mode pulse duration: No
Pulse energy: 1 – 20 mJ @ 266 - 800 nm

Max energy adjustment factor: 4.2
Low charge mode: No

CXI

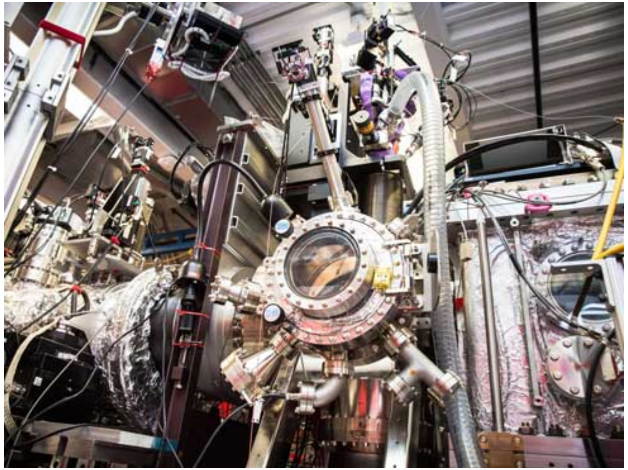

Coherent X-ray imaging

Brilliant hard X-ray pulses for coherent diffractive imaging (CDI). Ultra short pulses for "Diffraction-Before-Destruction" experiments.

Photon energy: 5 – 12 keV
Pulse duration: 40 – 300 fs
Low charge mode pulse duration: <10 fs
Pulse energy: 1 – 3 mJ

Max energy adjustment factor: 2.4
Low charge mode: Yes

AMO

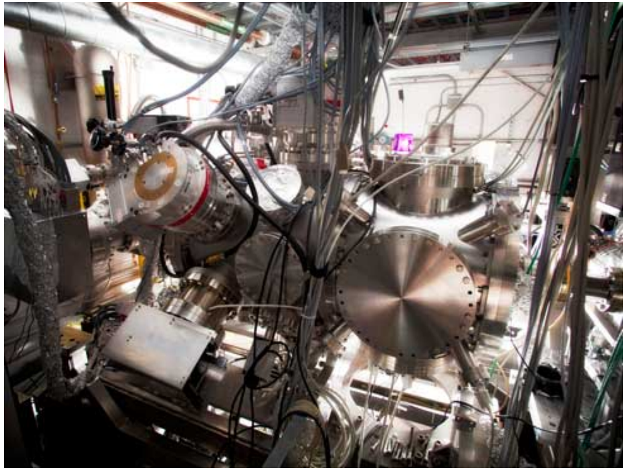

Atomic, Molecular & Optical Science

Soft X-rays for intense ultra short pulses. Gaseous targets of atoms, molecules, and nanoscale objects: protein crystals or viruses.

Photon energy: 0.48 – 2 keV
Pulse duration: 35 – 300 fs
Low charge mode pulse duration: No
Pulse energy: 1 – 20 mJ @ 266 - 800 nm

Max energy adjustment factor: 4.2
Low charge mode: No

CXI

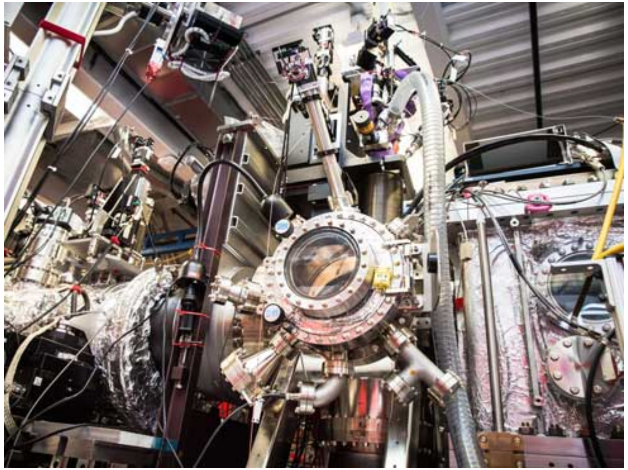

Coherent X-ray imaging

Brilliant hard X-ray pulses for coherent diffractive imaging (CDI). Ultra short pulses for "Diffraction-Before-Destruction" experiments.

Photon energy: 5 – 12 keV
Pulse duration: 40 – 300 fs
Low charge mode pulse duration: <10 fs
Pulse energy: 1 – 3 mJ

Max energy adjustment factor: 2.4
Low charge mode: Yes

MEC

Matter in Extreme Conditions

High peak brightness, ultra short pulses of tunable energy X-rays for studying the transient behavior of matter in extreme conditions.

Photon energy: 2.5 – 12 keV
Pulse duration: 10 – 300 fs
Low charge mode pulse duration: <10 fs
Pulse energy: 1 – 3 mJ

Max energy adjustment factor: 4.8
Low charge mode: Yes

AMO

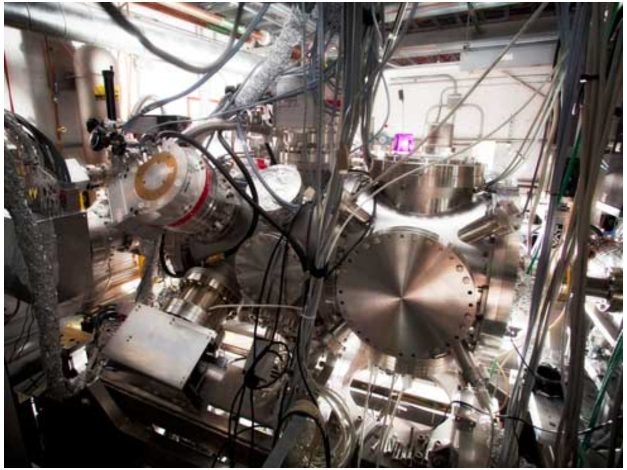

Atomic, Molecular & Optical Science

Soft X-rays for intense ultra short pulses. Gaseous targets of atoms, molecules, and nanoscale objects: protein crystals or viruses.

Photon energy: 0.48 – 2 keV
Pulse duration: 35 – 300 fs
Low charge mode pulse duration: No
Pulse energy: 1 – 20 mJ @ 266 - 800 nm

Max energy adjustment factor: 4.2
Low charge mode: No

CXI

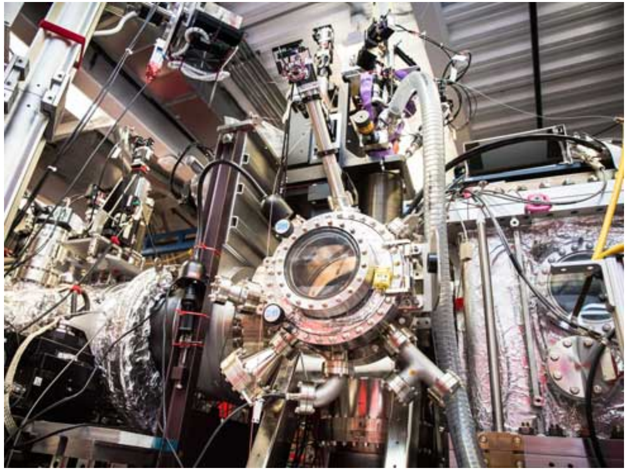

Coherent X-ray imaging

Brilliant hard X-ray pulses for coherent diffractive imaging (CDI). Ultra short pulses for "Diffraction-Before-Destruction" experiments.

Photon energy: 5 – 12 keV
Pulse duration: 40 – 300 fs
Low charge mode pulse duration: <10 fs
Pulse energy: 1 – 3 mJ

Max energy adjustment factor: 2.4
Low charge mode: Yes

MEC

Matter in Extreme Conditions

High peak brightness, ultra short pulses of tunable energy X-rays for studying the transient behavior of matter in extreme conditions.

Photon energy: 2.5 – 12 keV
Pulse duration: 10 – 300 fs
Low charge mode pulse duration: <10 fs
Pulse energy: 1 – 3 mJ

Max energy adjustment factor: 4.8
Low charge mode: Yes

Low charge mode: Lower charge per bunch allows for tighter compression without destroying the electron beam's phase space. Originally studying for accelerating 0.02 nC bunches instead of 1 nC.

Need to quickly switch between various beam/light parameters

No such look up table, or button exists

From the FAQ for users on the LCLS website:

1) What is the photon energy range which LCLS can provide and how long does it take to switch?

Factor of > 37

Answer :
(8/25/16) LCLS Machine Phys.
At present, the available photon energy range is 270 eV up to 10 keV. Photon energies as high as 12.8 keV may be reached with advanced notice and reduced reliability.

Energy changes can require anywhere from 5 minutes (small energy adjustments of 5-50%) to 45 minutes (energy adjustments of a factor of 2-3). In addition, some accelerator tuning may be required in order to re-establish the full x-ray pulse energy (e.g., to achieve more than 2 mJ may require another hour or more). This retuning is generally faster when the energy is increased rather than decreased. Please ask the operator for a time estimate when requesting photon energy changes.

A. Marinelli et al., "High-intensity double-pulse X-ray free-electron laser." Nature Communications, 2015. DOI: 10.1038/ncomms7369

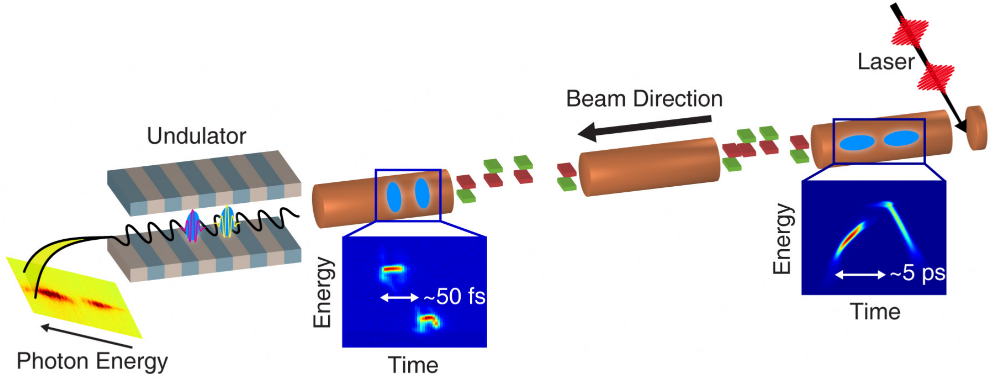

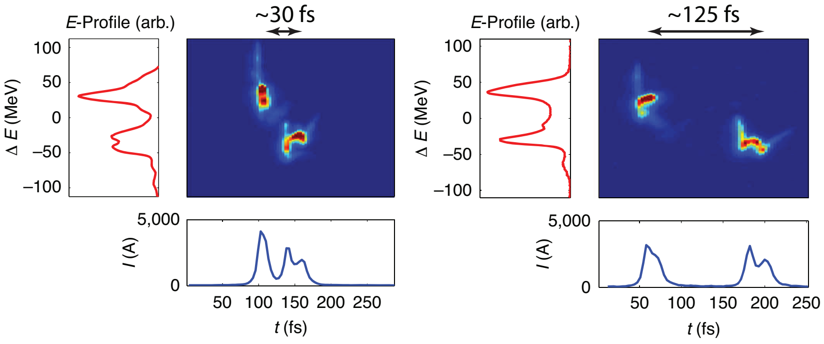

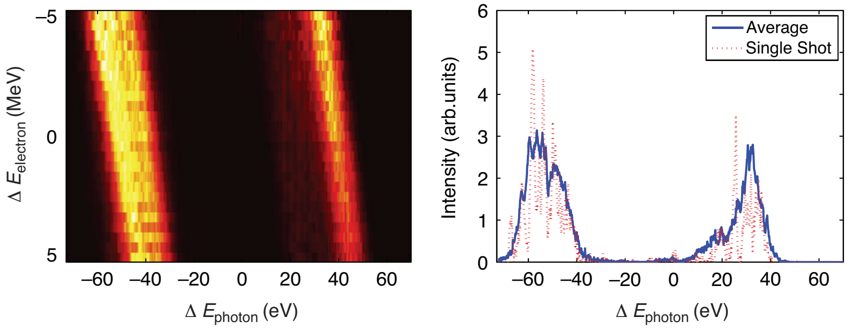

LCLS-II

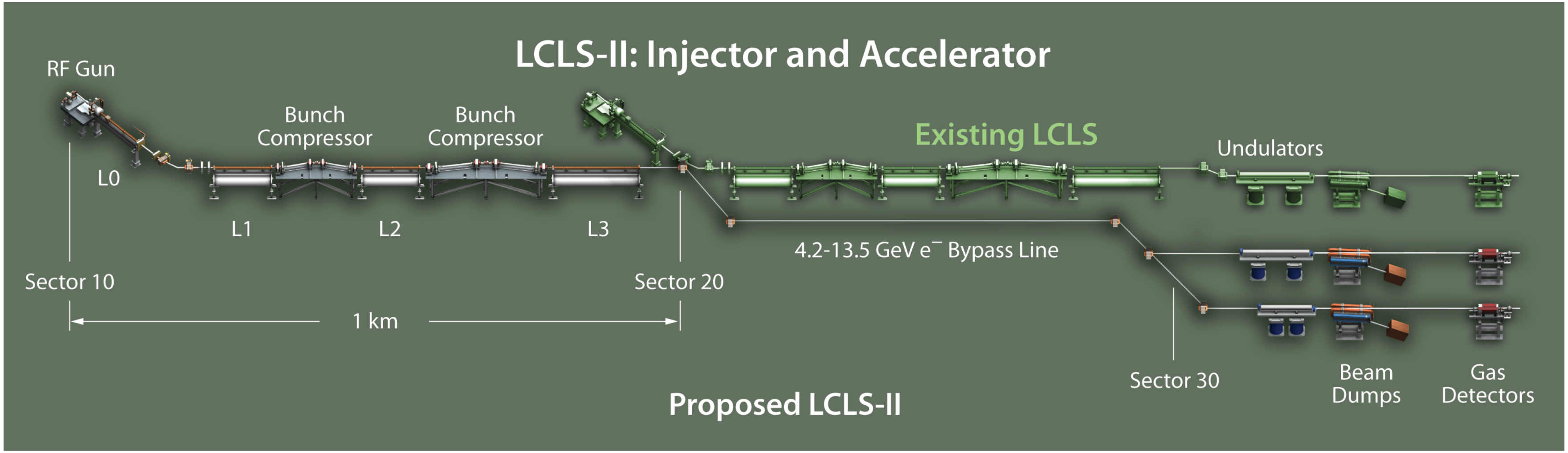
LCLS-II: Injector and Accelerator
RF Gun
Bunch Compressor
Bunch Compressor
Existing LCLS
Undulators
L0
L1
L2
L3
4.2-13.5 GeV e⁻ Bypass Line
Sector 10
Sector 20
1 km
Sector 30
Beam Dumps
Gas Detectors
Proposed LCLS-II

European XFEL

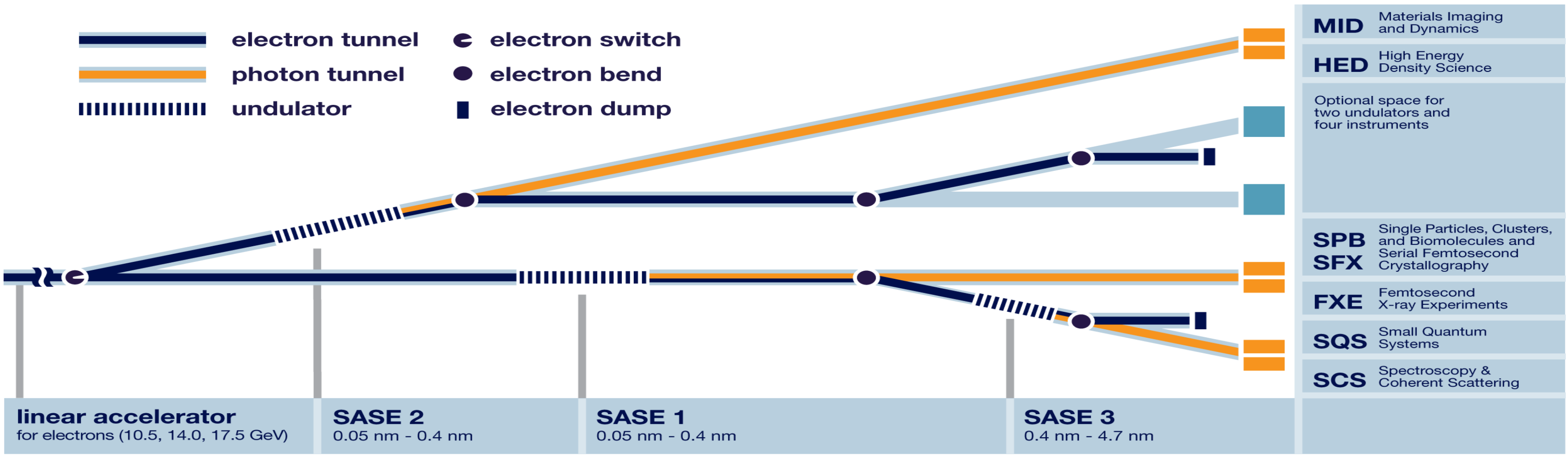

17.5 GeV electrons

Photon energy: 0.25 – 25 keV

27000 pulses/second

MaRIE

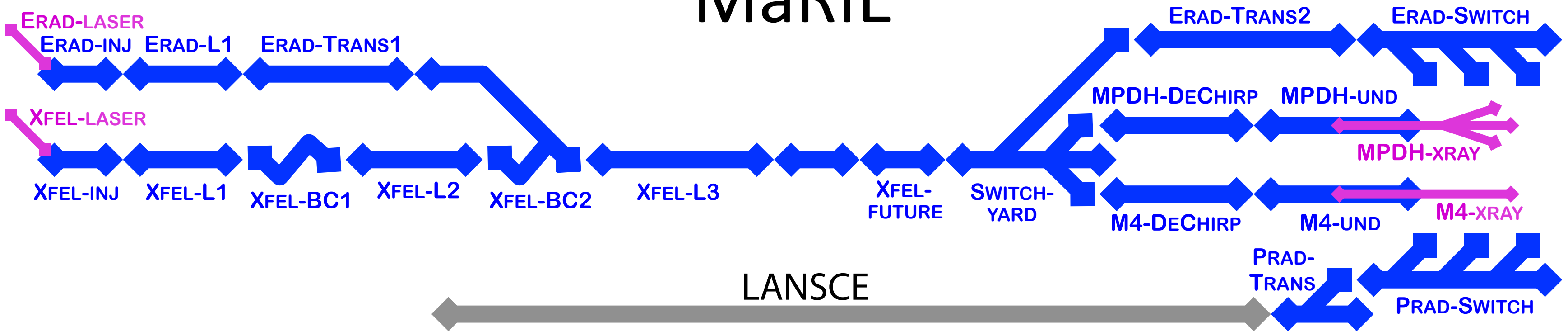

ERAD-LASER
ERAD-INJ
ERAD-L1
ERAD-TRANS1
XFEL-LASER
XFEL-INJ
XFEL-L1
XFEL-BC1
XFEL-L2
XFEL-BC2
XFEL-L3
XFEL-FUTURE
SWITCH-YARD
ERAD-TRANS2
ERAD-SWITCH
MPDH-DECHIRP
MPDH-UND
MPDH-XRAY
M4-DECHIRP
M4-UND
M4-XRAY
PRAD-TRANS
PRAD-SWITCH
LANSCE

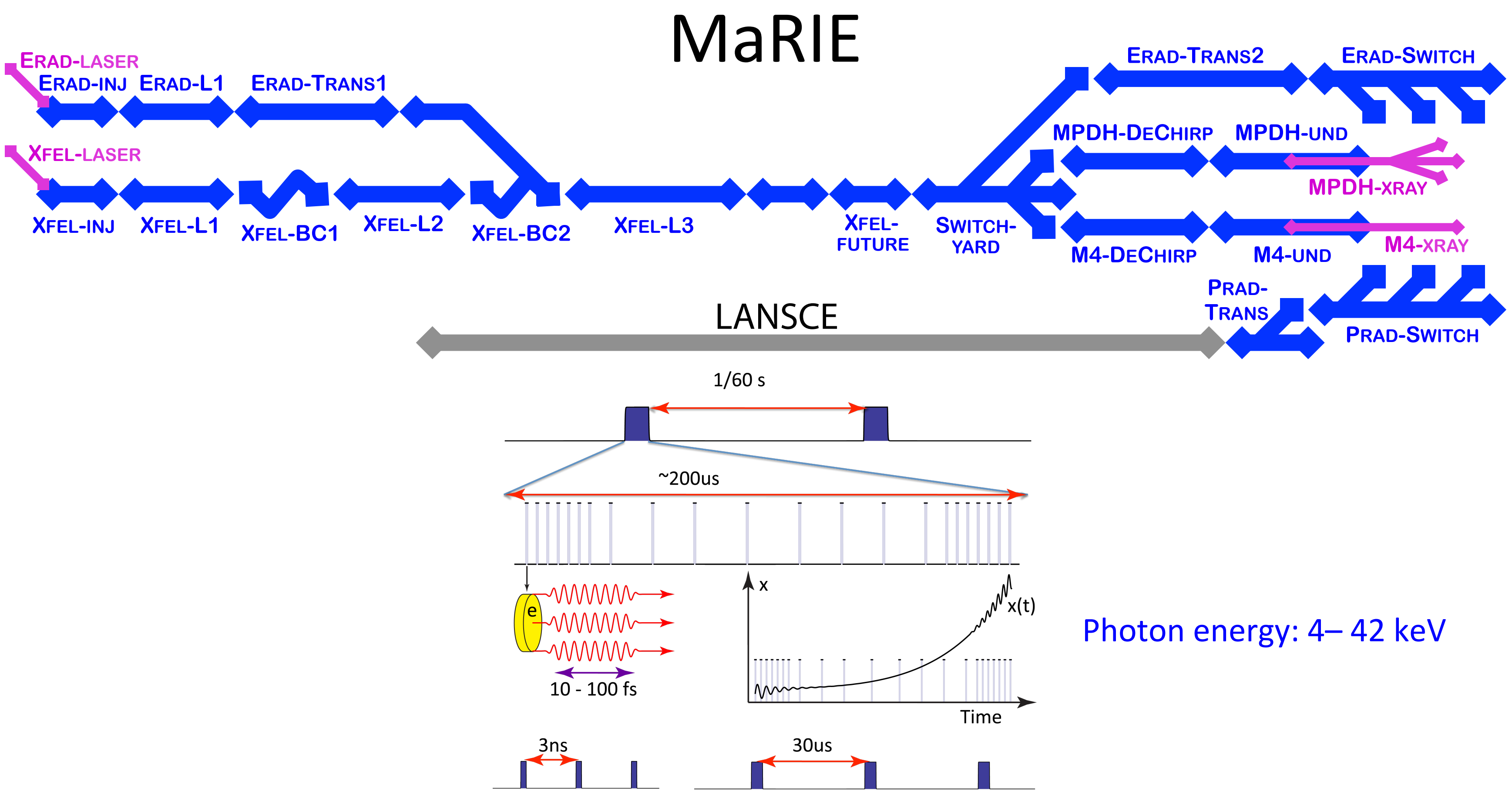

MaRIE
ERAD-LASER
ERAD-INJ
ERAD-L1
ERAD-TRANS1
XFEL-LASER
XFEL-INJ
XFEL-L1
XFEL-BC1
XFEL-L2
XFEL-BC2
XFEL-L3
XFEL-FUTURE
SWITCH-YARD
ERAD-TRANS2
ERAD-SWITCH
MPDH-DECHIRP
MPDH-UND
MPDH-XRAY
M4-DECHIRP
M4-UND
M4-XRAY
PRAD-TRANS
PRAD-SWITCH
LANSCE
1/60 s
~200us
e
10 - 100 fs
x
x(t)
Time
3ns
30us
Photon energy: 4– 42 keV

Accelerator Tuning Challenges

- Dynamics of intense charged particle bunches dominated by:
    - **Components drift unpredictably with time, misalignments**

Accelerator Tuning Challenges

- Dynamics of intense charged particle bunches dominated by:
  - **Components drift unpredictably with time, misalignments**
    - **Uncertain and time varying electron bunch distribution off cathode**
  - **Complex collective effects:**

@ FAST

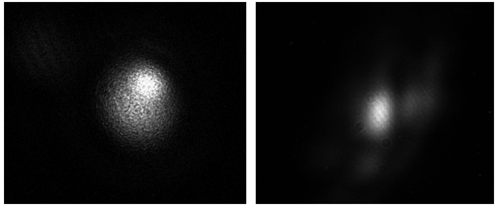

Example images of laser spot
(10 Aug. 2016, 11 Nov. 2017)

Accelerator Tuning Challenges

- Dynamics of intense charged particle bunches dominated by:
  - **Components drift unpredictably with time, misalignments**
    - **Uncertain and time varying electron bunch distribution off cathode**
  - **Complex collective effects:**
    - **Wakefields**
    - **Space charge**
    - **Coherent synchrotron radiation**

@ FAST

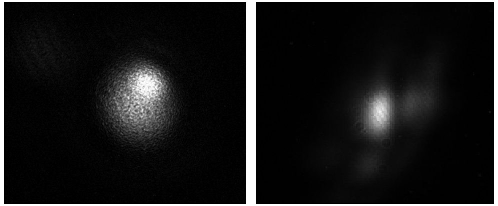

Example images of laser spot
(10 Aug. 2016, 11 Nov. 2017)

Accelerator Tuning Challenges

- Dynamics of intense charged particle bunches dominated by:
  - **Components drift unpredictably with time, misalignments**
    - **Uncertain and time varying electron bunch distribution off cathode**
  - **Complex collective effects:**
    - **Wakefields**
    - **Space charge**
    - **Coherent synchrotron radiation**
  - **Limited diagnostics**

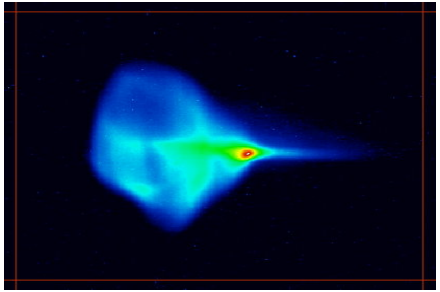

Typical 2D (x,y) beam profile, not a simple Gaussian.

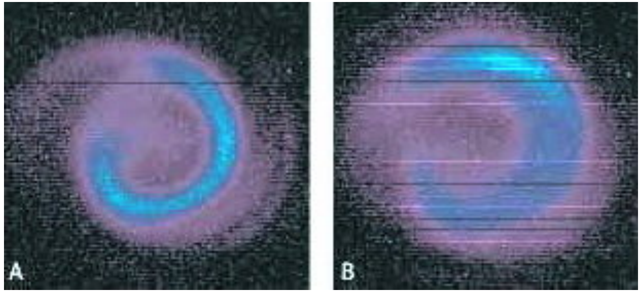

X_ray output from VISA XFEL at Brookhaven. Caused by shot-to-shot variation in transverse beam parameters, electron-beam alignment fluctuations.

@ FAST

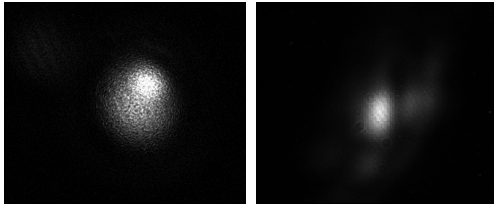

Example images of laser spot (10 Aug. 2016, 11 Nov. 2017)

Robust model-based control at Swiss FEL

Rezaeizadeh, Amin, Thomas Schilcher, and Roy S. Smith. "Control of the Swiss Free Electron Laser: Methods for Precision Control of Pulsed-Mode Accelerator Beams." *IEEE Control Systems* 37.6 (2017): 30-51.

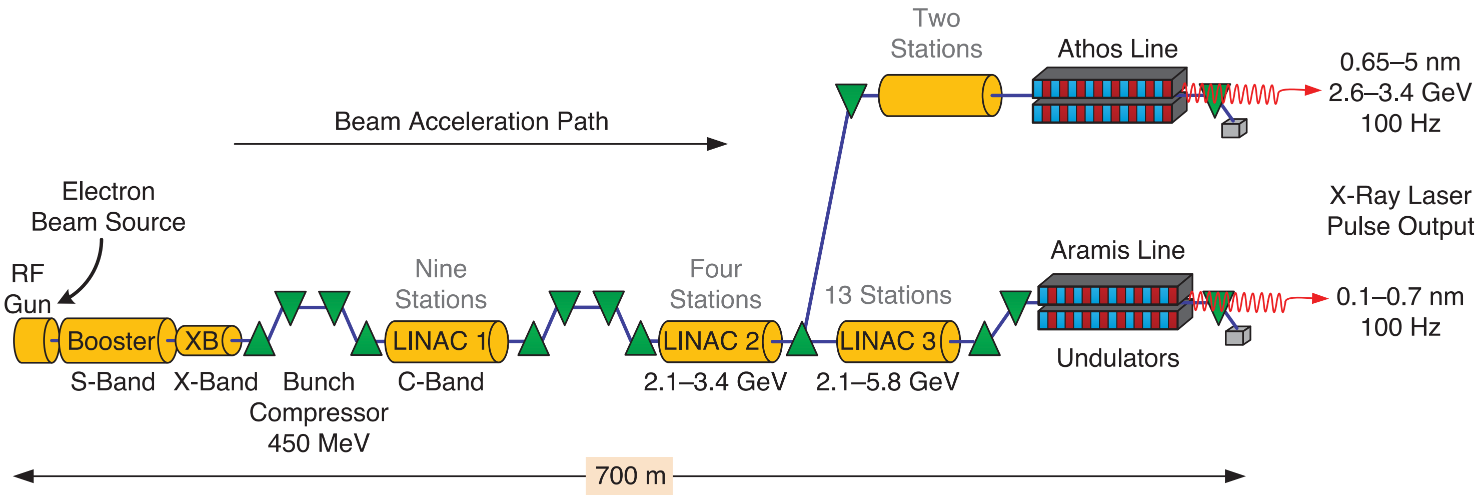

Rezaeizadeh, Amin, Thomas Schilcher, and Roy S. Smith. "Control of the Swiss Free Electron Laser: Methods for Precision Control of Pulsed-Mode Accelerator Beams." *IEEE Control Systems* 37.6 (2017): 30-51.

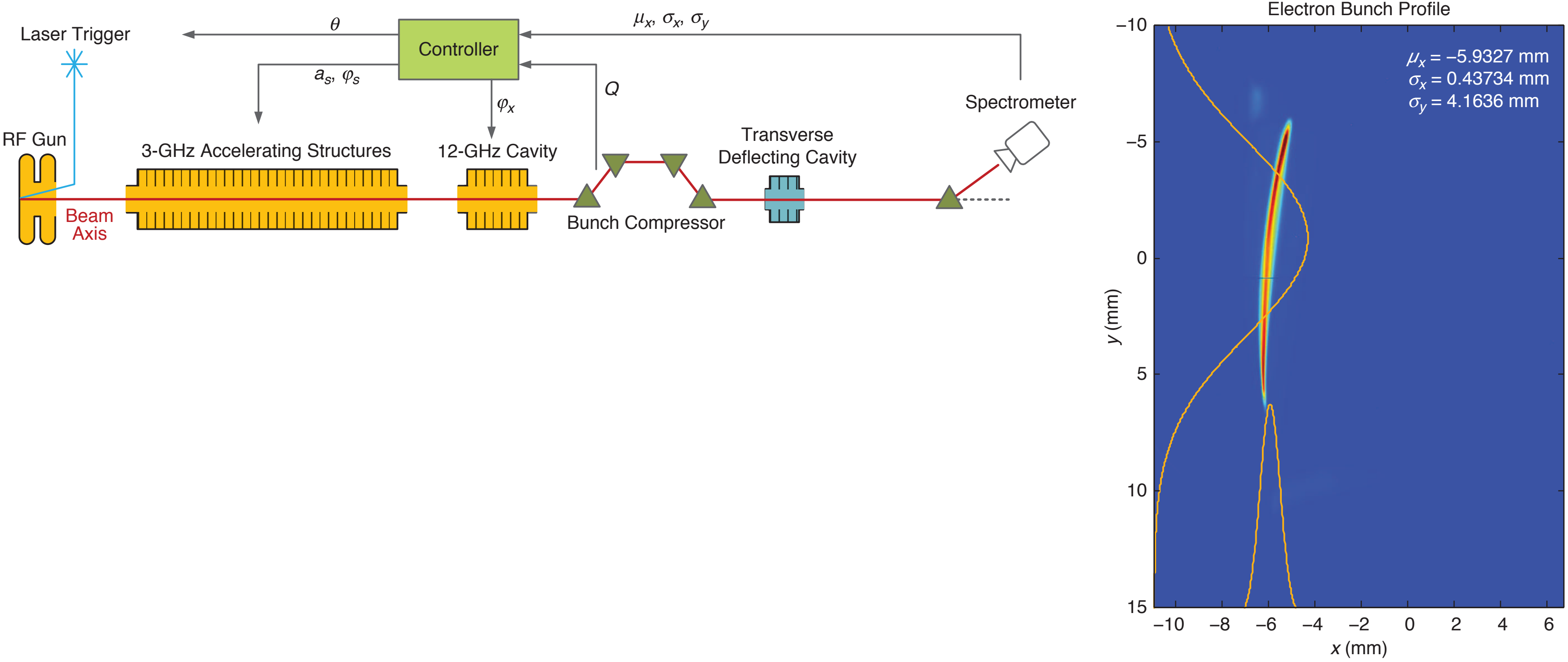

Rezaeizadeh, Amin, Thomas Schilcher, and Roy S. Smith. "Control of the Swiss Free Electron Laser: Methods for Precision Control of Pulsed-Mode Accelerator Beams." *IEEE Control Systems* 37.6 (2017): 30-51.

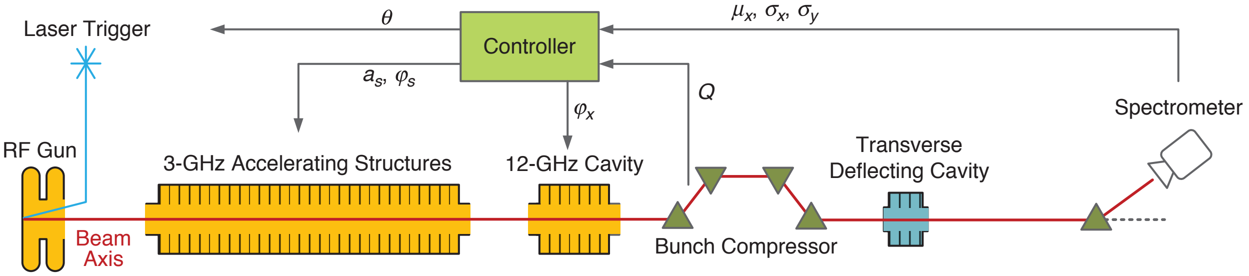

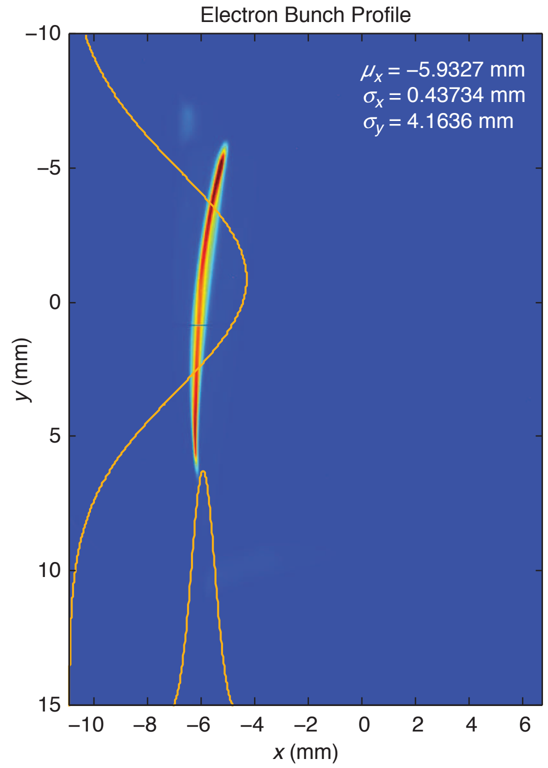

$$y = [Q \quad \mu_x \quad \sigma_x \quad \sigma_y], \qquad u = [\theta \quad a_s \quad \varphi_s \quad \varphi_x]$$

$$y = f(u), \quad y - y_0 \approx R(u - u_0)$$

$$u_{k+1} = u_k + \gamma R^{-1}(y^{\text{ref}} - y_k)$$

Very sensitive to uncertainty in R, especially for poorly conditioned matrix.

Rezaeizadeh, Amin, Thomas Schilcher, and Roy S. Smith. "Control of the Swiss Free Electron Laser: Methods for Precision Control of Pulsed-Mode Accelerator Beams." *IEEE Control Systems* 37.6 (2017): 30-51.

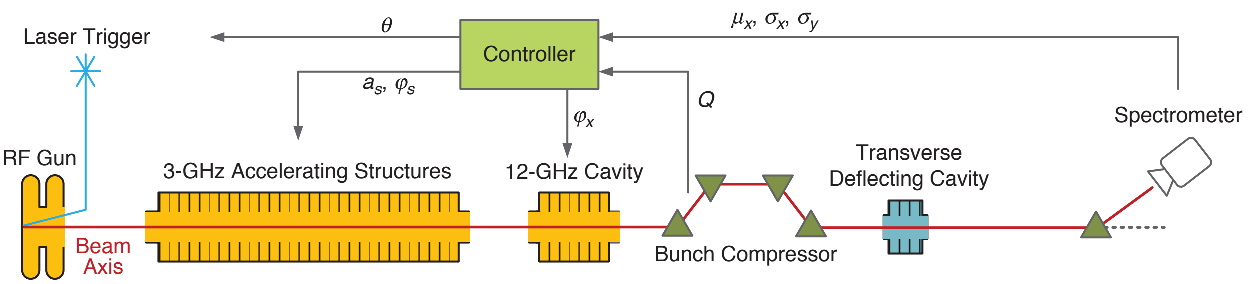

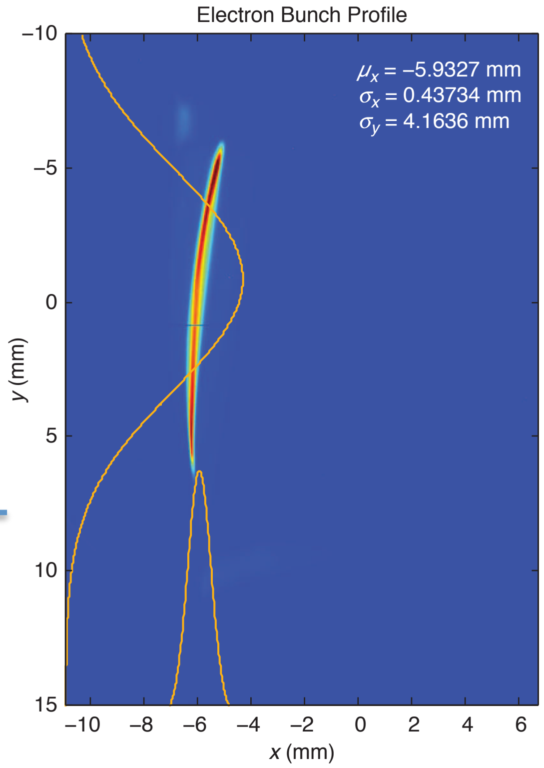

$$y = [Q \quad \mu_x \quad \sigma_x \quad \sigma_y], \qquad u = [\theta \quad a_s \quad \varphi_s \quad \varphi_x]$$

$$y = f(u), \quad y - y_0 \approx R(u - u_0)$$

$$u_{k+1} = u_k + \gamma R^{-1}(y^{\text{ref}} - y_k)$$

$$u_0 = \text{argmin}_u \left\{ \left\| y^{\text{ref}} - R_{nom} u \right\|_2 + \gamma \left\| R_{nom} \right\|_2 \left\| u \right\|_2 \right\}$$

Robust control

$$R = R_{nom}(I_m + \Delta), \quad \|\Delta\|_2 \leq 1$$

$$\Delta_k = \text{argmin}_\Delta \left\{ \| y_k - R_{nom}(I_m + \Delta) u_k \|_2 \right\}$$

$$u_{k+1} = \text{argmin}_\Delta \left\{ \left\| y^{\text{ref}} - R_{nom}(I_m + \Delta_k) u \right\|_2 \right\}, \quad \|u\|_2 < u_{max}, \quad \|u - u_k\|_2 < \delta_{max}$$

Rezaeizadeh, Amin, Thomas Schilcher, and Roy S. Smith. "Control of the Swiss Free Electron Laser: Methods for Precision Control of Pulsed-Mode Accelerator Beams." *IEEE Control Systems* 37.6 (2017): 30-51.

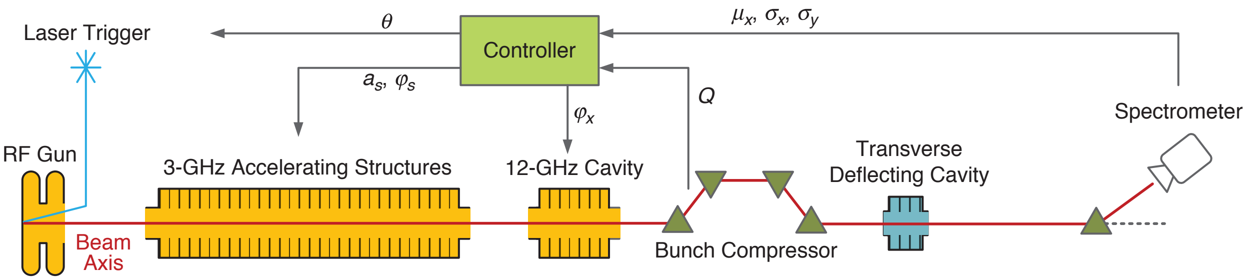

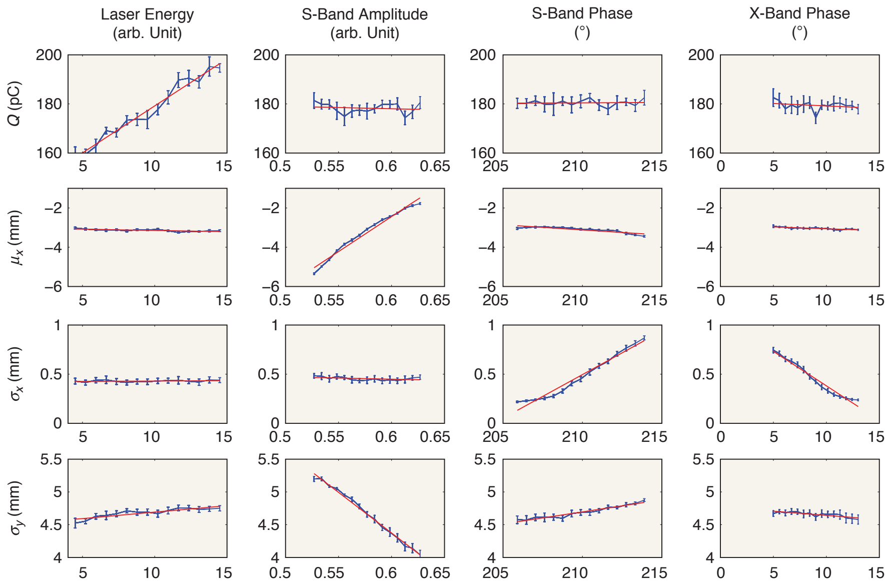

Learning the response matrix, R

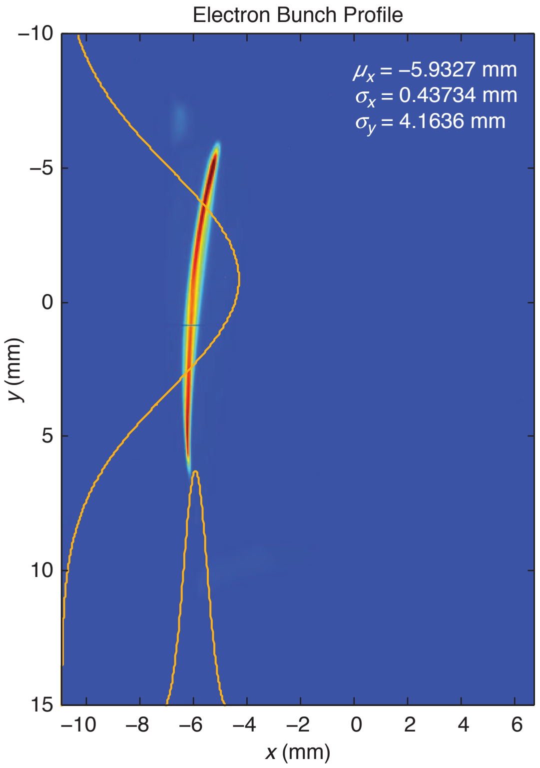

Rezaeizadeh, Amin, Thomas Schilcher, and Roy S. Smith. "Control of the Swiss Free Electron Laser: Methods for Precision Control of Pulsed-Mode Accelerator Beams." *IEEE Control Systems* 37.6 (2017): 30-51.

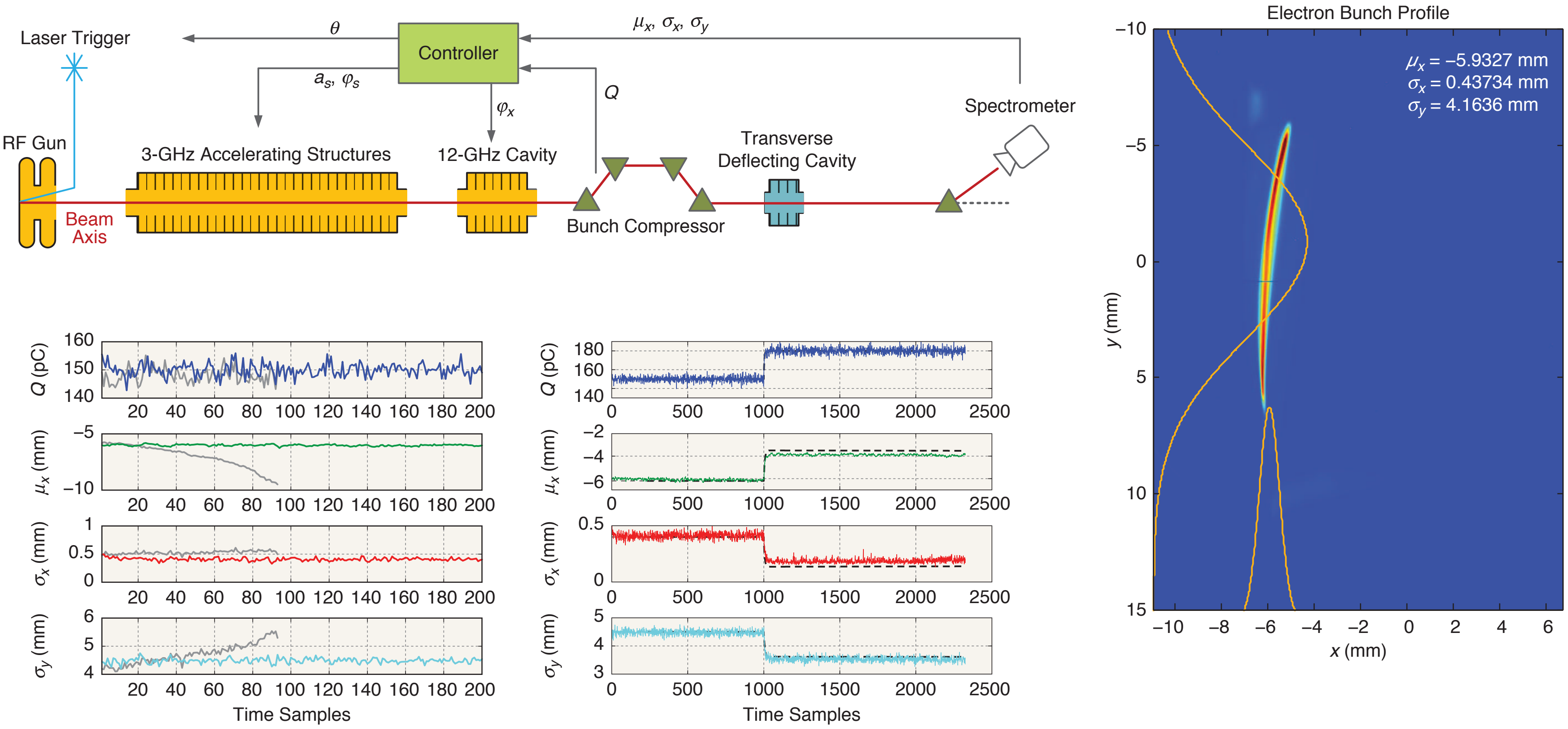

Robust model-based control at Swiss FEL

- Beam control
- RF pulse flattening
- Electron orbit control
- Laser pulse-stacking for flat-topped pulse shapes

- R locally estimated for each operating region?
- Will each R have to be re-computed periodically?
- Increasing numbers of parameters >> longer data scans?

Machine Learning Approaches

ML for improvement of diagnostics

Detection of faulty BPMs at CERN (1024 BPMs) > Cluster analysis, faulty signals should appear as outliers

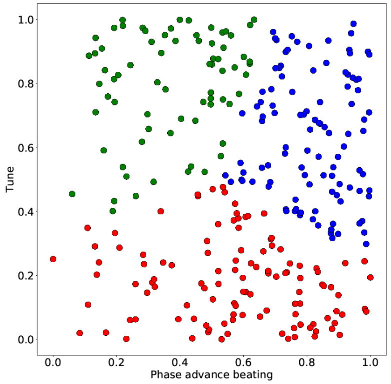

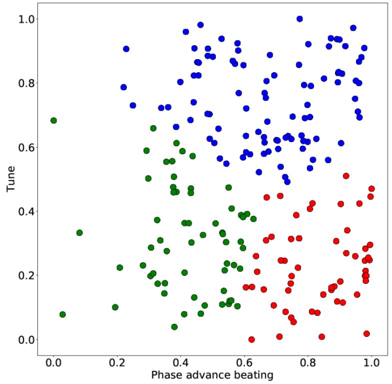

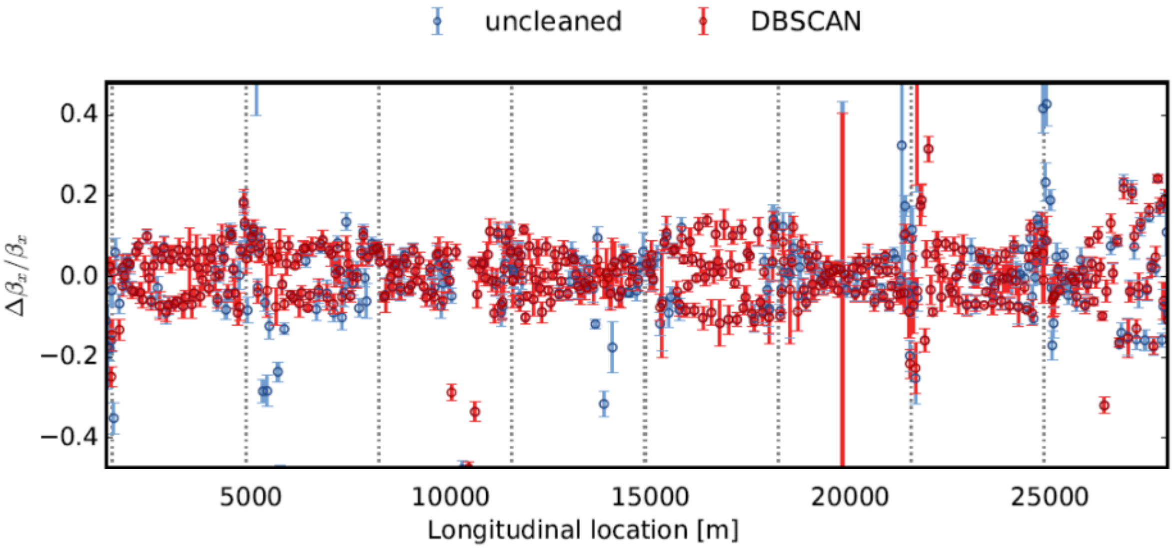

E. Fol and Tomas Garcia, Detection of faulty Beam Position Monitors at CERN
Machine Learning Applications for Particle Accelerators, Feb. 28 – March 2, 2018,
SLAC National Accelerator Laboratory

NN-based model for automatic FEL tuning

Compact, THz FEL design based on previously operational TEU-FEL

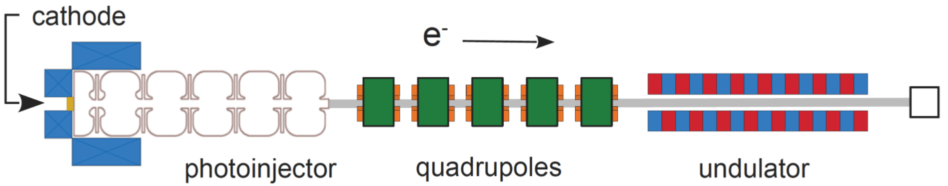

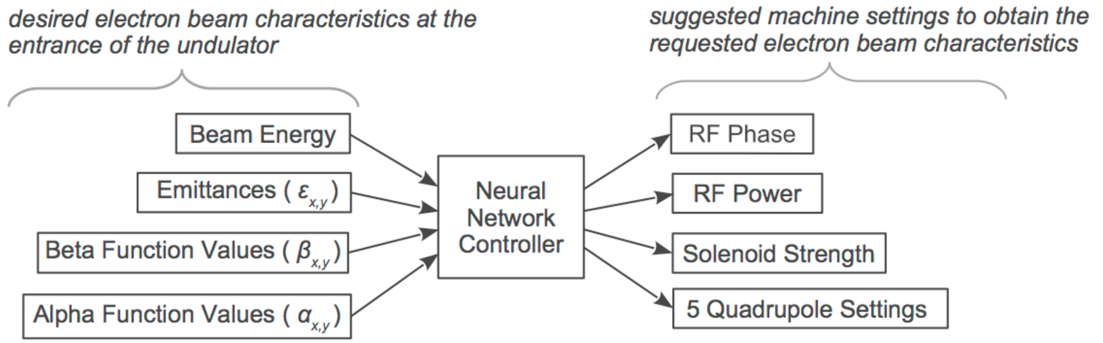

3 – 6 MeV electron beam
200 – 800 µm photon beam

Previously operated at University of Twente in the Netherlands

Was going to be re-built at CSU: have simulation from design studies

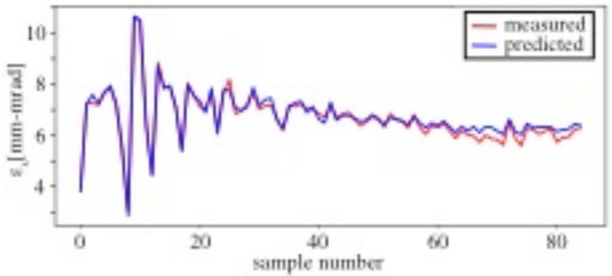

ML methods for shot-to-shot spectral profiling of FEL light

Machine learning applied to single-shot x-ray diagnostics in an XFEL

A. Sanchez-Gonzalez,[1] P. Micaelli,[1] C. Olivier,[1] T. R. Barillot,[1] M. Ilchen,[2,3] A. A. Lutman,[4] A. Marinelli,[4] T. Maxwell,[4] A. Achner,[3] M. Agåker,[5] N. Berrah,[6] C. Bostedt,[4,7] J. Buck,[8] P. H. Bucksbaum,[2,9] S. Carron Montero,[4,10] B. Cooper,[1] J. P. Cryan,[2] M. Dong,[5] R. Feifel,[11] L. J. Frasinski,[1] H. Fukuzawa,[12] A. Galler,[3] G. Hartmann,[8,13] N. Hartmann,[4] W. Helml,[4,14] A. S. Johnson,[1] A. Knie,[13] A. O. Lindahl,[2,11] J. Liu,[3] K. Motomura,[12] M. Mucke,[5] C. O'Grady,[4] J-E. Rubensson,[5] E. R. Simpson,[1] R. J. Squibb,[11] C. Såthe,[15] K. Ueda,[12] M. Vacher,[16,17] D. J. Walke,[1] V. Zhaunerchyk,[11] R. N. Coffee,[4] and J. P. Marangos[1]

A. Sanchez-Gonzalez, et al. https://arxiv.org/pdf/1610.03378.pdf

- Used archived data to learn correlation between fast and slow diagnostics

Shot-to-shot data: **Current profiles, BPMs, X-ray gas detectors**

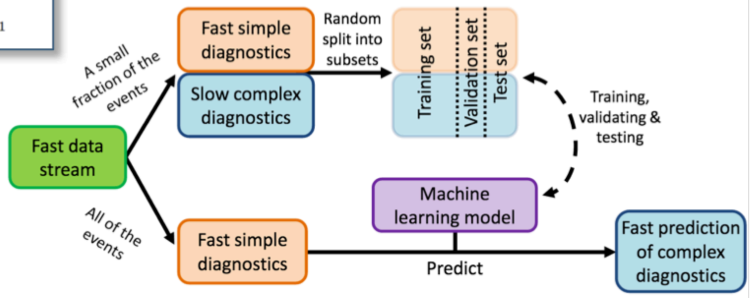

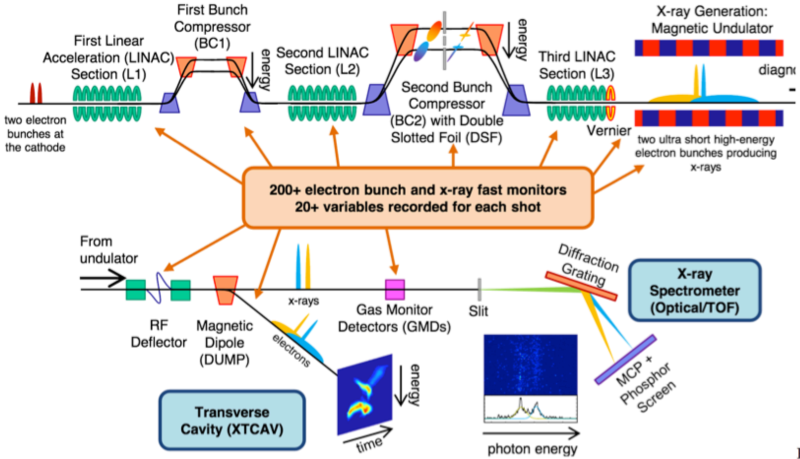

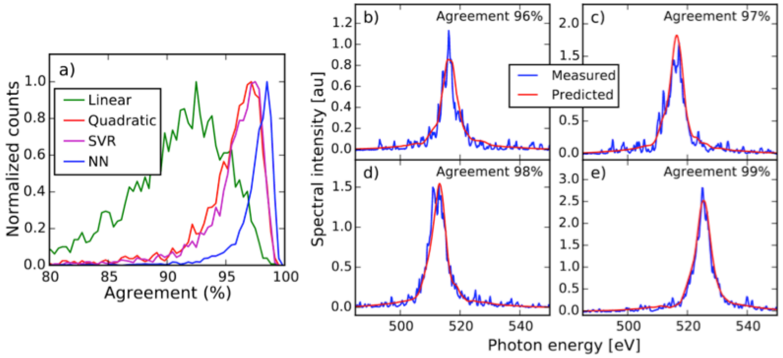

FIG. 4. Spectral shape prediction for a single pulse. (a) Histogram of agreements between the predicted and the measured spectra for the test set using the 4 different models. (b-e) Examples of the measured and the predicted spectra using a neural network to illustrate the accuracy for different agreement values.

Machine Learning Approaches
(mostly statistics and big data so far)

Machine Learning Approaches

(mostly statistics and big data so far)

Automatic Feedback for in-hardware Tuning and Optimization

FERMI: Optimization Through Correlation Minimization
- Giulio Gaio, IFCA Machine Learning Workshop, SLAC, 03/02/2018

- Automatic optimization of the temporal overlap between seed laser pulse and electron bunch (1 variable)
- Correlation between the electron bunch arrival time (*sensor*) and the FEL energy (*target*)
- The actuator is a mechanical delay line (slit) on the seed laser path

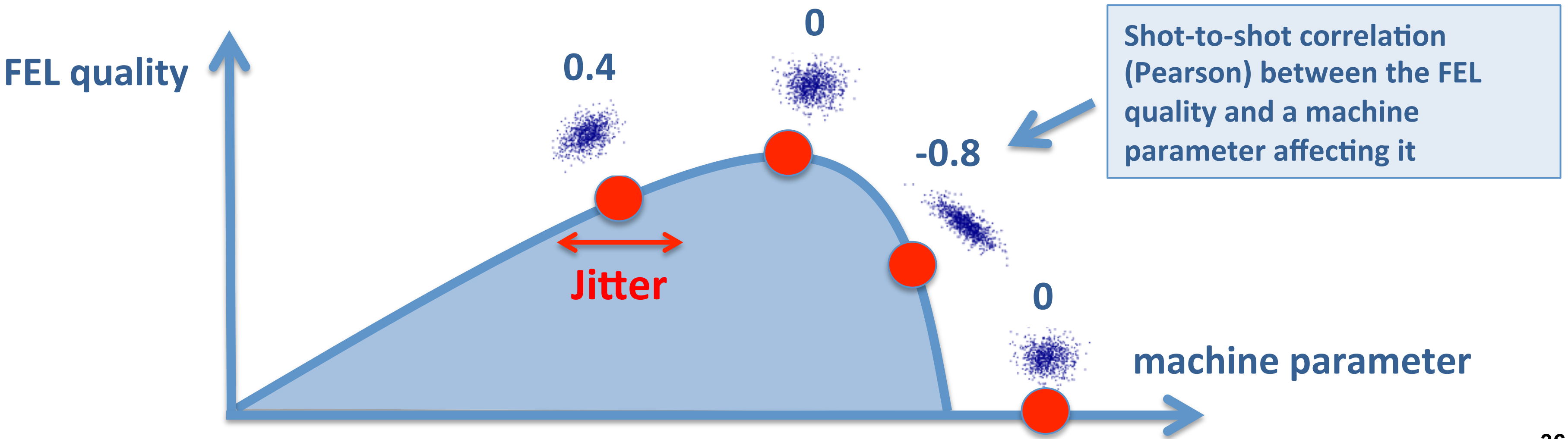

FERMI: Optimization Through Correlation Minimization
- Giulio Gaio, IFCA Machine Learning Workshop, SLAC, 03/02/2018

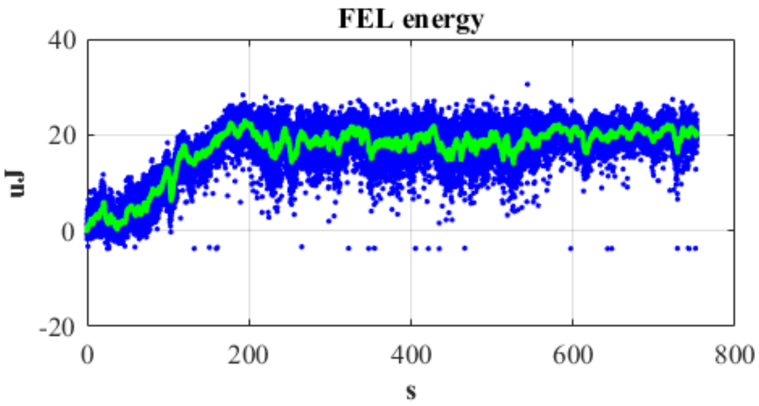

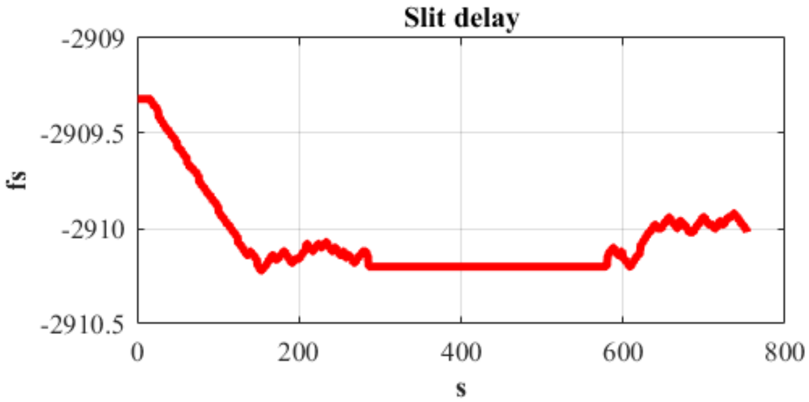

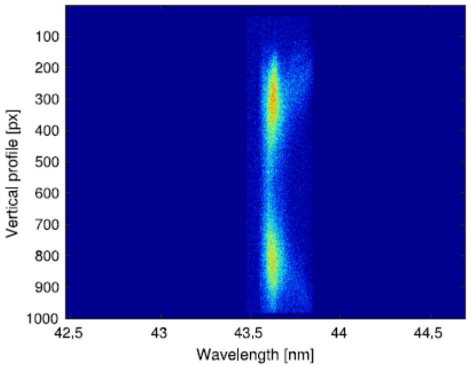

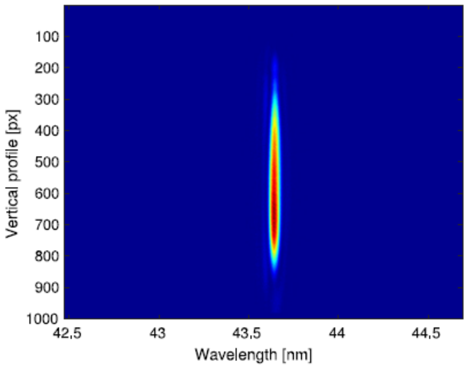

The **FEL Quality Factor** (*FELQFactor*): index which summarizing, in a number, the **most important features of the photon energy spectrum**: intensity, spectral purity and number of modes.

Actuator: seed laser delay line.

"Free-electron Laser Spectrum Evaluation and Automatic Optimization", Nuclear Inst. and Methods in Physics Research, A 871 (2017) 20 29

OCELT at EUXFEL

Generic optimizer: SASE optimization

- Air coils between the undulator cells were used to optimize the SASE signal
- Up to 6 air coils are typically used at the same time.

Nelder-Mead (simplex) and conjugate gradient (CG) method

- Limited to ~6 parameters
- Won’t work with large hysteresis
- Won’t work with time-varying system

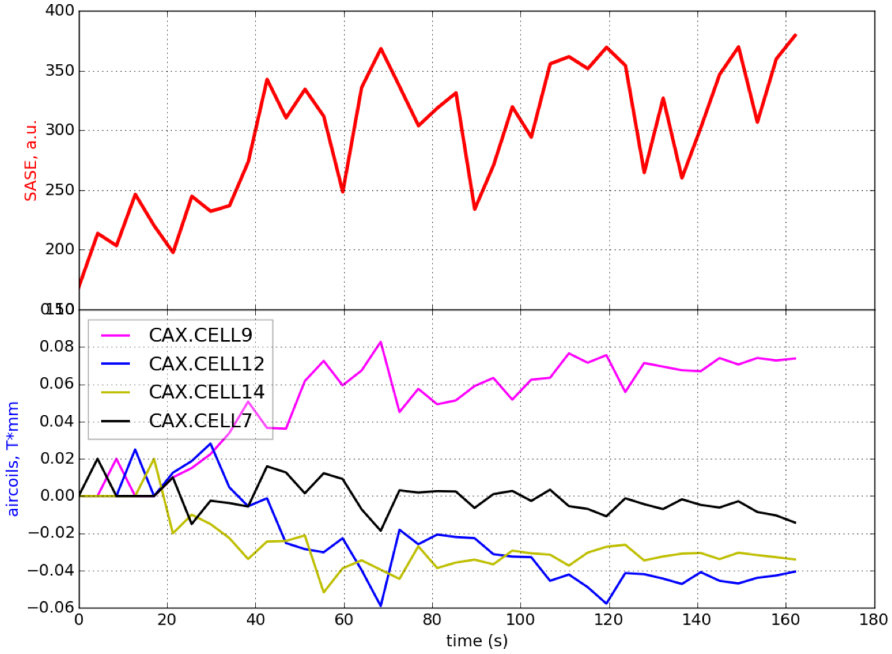

S. Tomin, Machine Learning Applications for Particle Accelerators, SLAC ML Workshop
I. Agapov et al., Automatic tuning of Free Electron Lasers, arXiv:1704.02335v1

Tuning Method Currently Being Developed at LANL

Extremum Seeking

Model-independent feedback

- Noisy and time varying systems
- Many coupled parameters

Bounded Extremum Seeking: Model-Independent Tuning and Optimization

A. Scheinker and D. Scheinker, "Extremum Seeking with Discontinuous Dithers," *Automatica*, vol. 69, pp. 250-257, 2016.
A. Scheinker and D. Scheinker, "Extremum Seeking for Stabilization of Systems not Affine in Control," 2017.

$$\begin{bmatrix} \dot{x}_1 \\ \vdots \\ \dot{x}_n \end{bmatrix} = \dot{\mathbf{x}} = \mathbf{f}(\mathbf{x}, \mathbf{p}, t) = \begin{bmatrix} f_1(x_1, \ldots, x_n, p_1, \ldots, p_m, t) \\ \vdots \\ f_n(x_1, \ldots, x_n, p_1, \ldots, p_m, t) \end{bmatrix}$$

Bounded Extremum Seeking: Model-Independent Tuning and Optimization

$$\begin{bmatrix} \dot{x}_1 \\ \vdots \\ \dot{x}_n \end{bmatrix} = \dot{\mathbf{x}} = \mathbf{f}(\mathbf{x}, \mathbf{p}, t) = \begin{bmatrix} f_1(x_1, \dots, x_n, p_1, \dots, p_m, t) \\ \vdots \\ f_n(x_1, \dots, x_n, p_1, \dots, p_m, t) \end{bmatrix}$$

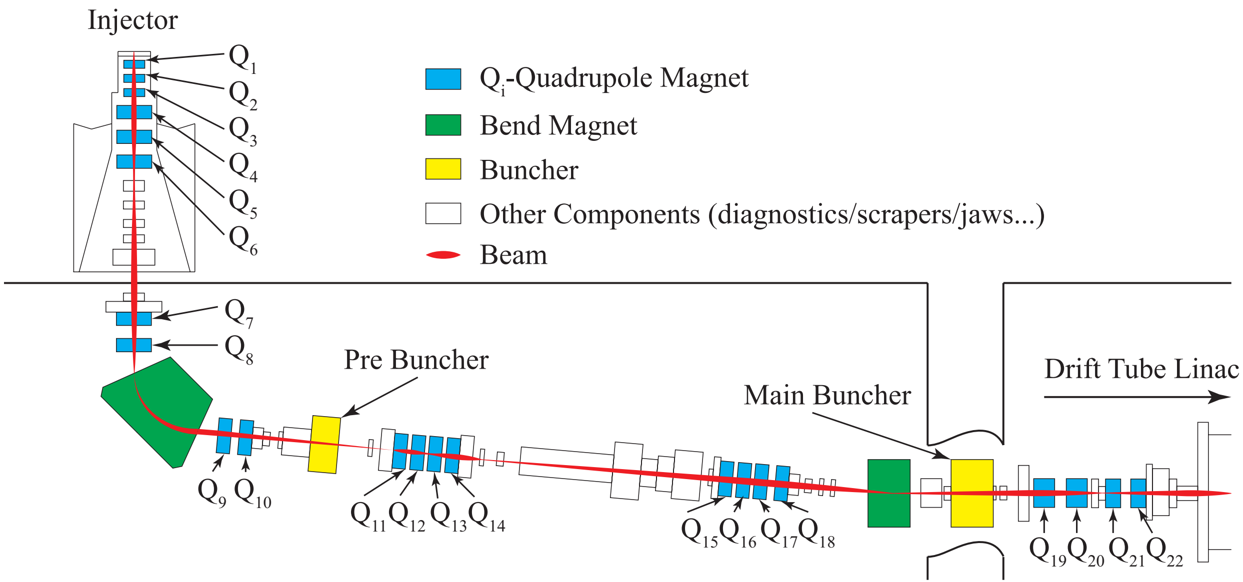

Bounded Extremum Seeking: Model-Independent Tuning and Optimization

$$\begin{bmatrix} \dot{x}_1 \\ \vdots \\ \dot{x}_n \end{bmatrix} = \dot{\mathbf{x}} = \mathbf{f}(\mathbf{x}, \mathbf{p}, t) = \begin{bmatrix} f_1(x_1, \ldots, x_n, p_1, \ldots, p_m, t) \\ \vdots \\ f_n(x_1, \ldots, x_n, p_1, \ldots, p_m, t) \end{bmatrix}$$

$$p_1(t) = Q_1 \text{ current}$$

$$\vdots$$

$$p_m(t) = Q_m \text{ current}$$

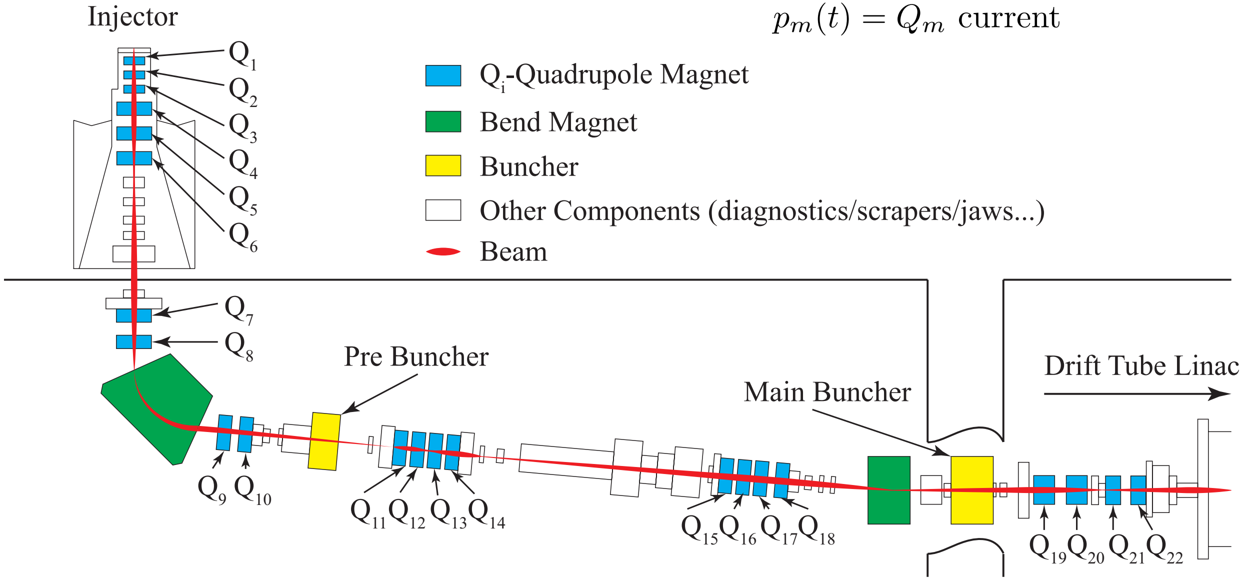

Bounded Extremum Seeking: Model-Independent Tuning and Optimization

$$\begin{bmatrix} \dot{x}_1 \\ \vdots \\ \dot{x}_n \end{bmatrix} = \dot{\mathbf{x}} = \mathbf{f}(\mathbf{x}, \mathbf{p}, t) = \begin{bmatrix} f_1(x_1, \ldots, x_n, p_1, \ldots, p_m, t) \\ \vdots \\ f_n(x_1, \ldots, x_n, p_1, \ldots, p_m, t) \end{bmatrix}$$

$$p_1(t) = Q_1 \text{ current}$$
$$\vdots$$
$$p_m(t) = Q_m \text{ current}$$

$$x_1(t) = X_{\text{rms}}(\text{position } 1)$$
$$x_2(t) = Y_{\text{rms}}(\text{position } 1)$$
$$\vdots$$
$$x_n(t) = X_{\text{rms}}(\text{position n})$$

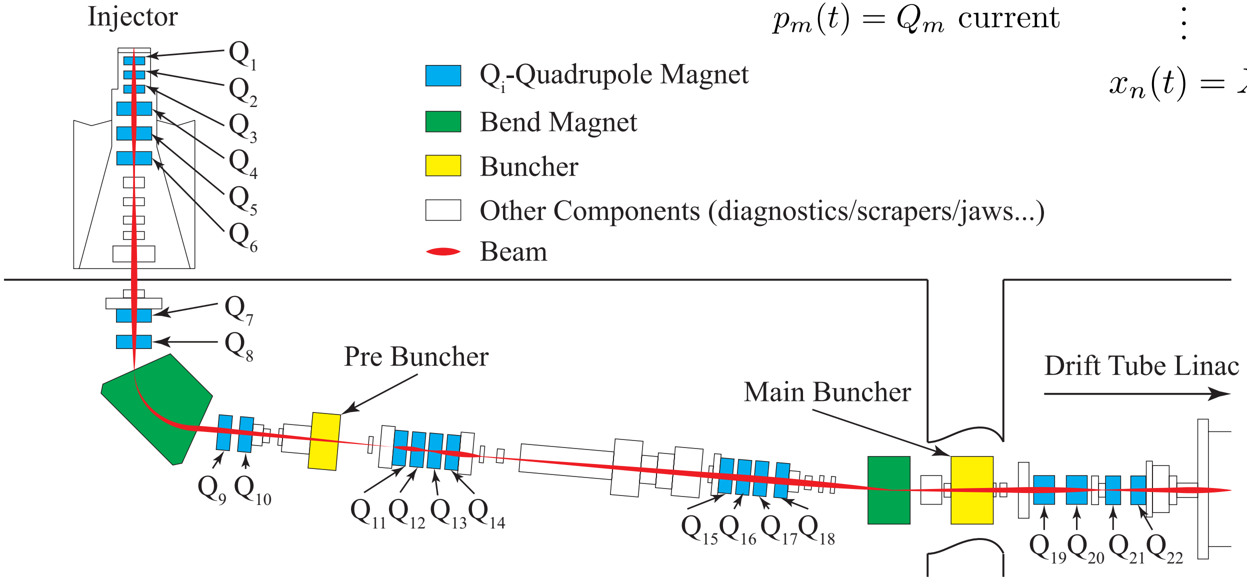

Bounded Extremum Seeking: Model-Independent Tuning and Optimization

$$\begin{bmatrix} \dot{x}_1 \\ \vdots \\ \dot{x}_n \end{bmatrix} = \dot{\mathbf{x}} = \mathbf{f}(\mathbf{x}, \mathbf{p}, t) = \begin{bmatrix} f_1(x_1, \ldots, x_n, p_1, \ldots, p_m, t) \\ \vdots \\ f_n(x_1, \ldots, x_n, p_1, \ldots, p_m, t) \end{bmatrix}$$

$$y = V(\mathbf{x}, t) + n(t)$$

noise

$$y = (I(t) - I_0)^2 + n(t)$$

Surviving beam current at end.

$$p_1(t) = Q_1 \text{ current}$$
$$\vdots$$
$$p_m(t) = Q_m \text{ current}$$

$$x_1(t) = X_{\text{rms}}(\text{position } 1)$$
$$x_2(t) = Y_{\text{rms}}(\text{position } 1)$$
$$\vdots$$
$$x_n(t) = X_{\text{rms}}(\text{position n})$$

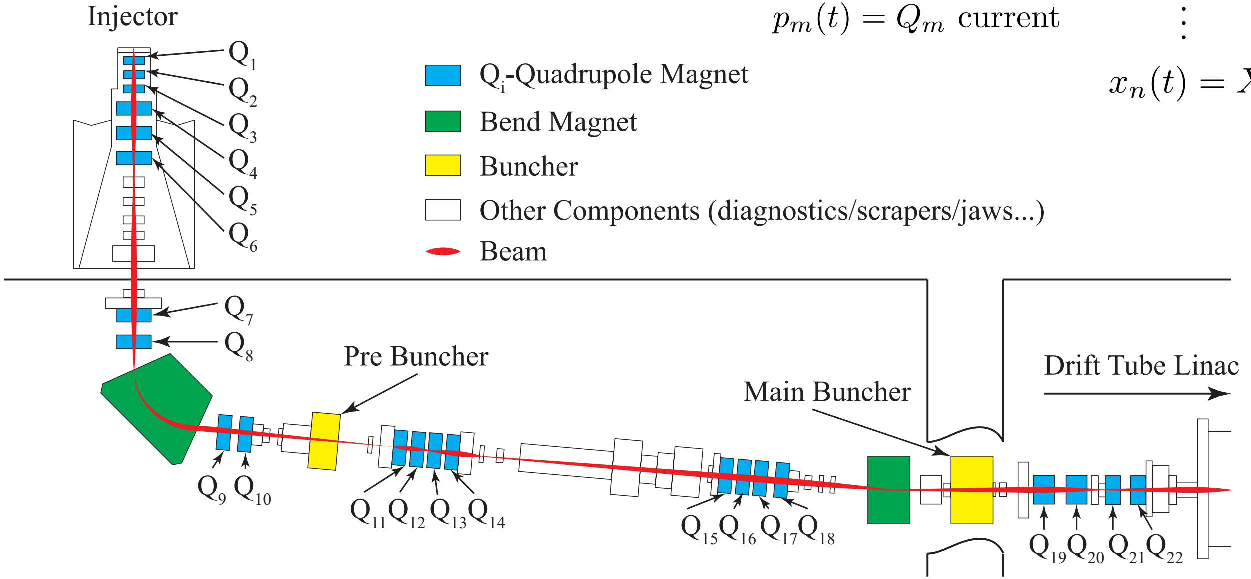

$$y = V(\mathbf{x}, t) + n(t)$$

$$\begin{bmatrix} \dot{x}_1 \\ \vdots \\ \dot{x}_n \end{bmatrix} = \dot{\mathbf{x}} = \mathbf{f}(\mathbf{x}, \mathbf{p}, t) = \begin{bmatrix} f_1(x_1, \ldots, x_n, p_1, \ldots, p_m, t) \\ \vdots \\ f_n(x_1, \ldots, x_n, p_1, \ldots, p_m, t) \end{bmatrix}$$

$$\frac{dp_1}{dt} = \sqrt{\alpha\omega_1}\cos(\omega_1 t + ky)$$

$$\frac{dp_2}{dt} = \sqrt{\alpha\omega_2}\cos(\omega_2 t + ky)$$

$$\frac{dp_3}{dt} = \sqrt{\alpha\omega_3}\cos(\omega_3 t + ky)$$

$$\vdots$$

$$\frac{dp_m}{dt} = \sqrt{\alpha\omega_m}\cos(\omega_m t + ky)$$

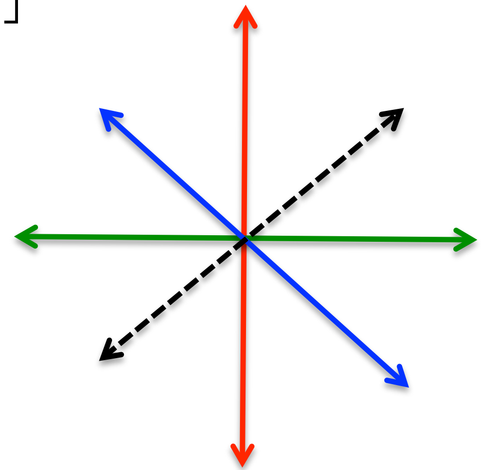

Dithering with different frequencies makes the parameters "perpendicular" in Hilbert space.

$$\omega_i = \omega r_i, \;\; r_i \neq r_j \implies \text{ for any } t > 0$$

$$\lim_{\omega \to \infty} \langle \cos(\omega_i t), \cos(\omega_j t) \rangle = \lim_{\omega \to \infty} \int_0^t \cos(\omega_i \tau)\cos(\omega_j \tau) d\tau = 0$$

$$\begin{bmatrix} \dot{x}_1 \\ \vdots \\ \dot{x}_n \end{bmatrix} = \dot{\mathbf{x}} = \mathbf{f}(\mathbf{x}, \mathbf{p}, t) = \begin{bmatrix} f_1(x_1, \ldots, x_n, p_1, \ldots, p_m, t) \\ \vdots \\ f_n(x_1, \ldots, x_n, p_1, \ldots, p_m, t) \end{bmatrix}$$

$$y = V(\mathbf{x}, t) + n(t)$$

$$\frac{dp_1}{dt} = \sqrt{\alpha\omega_1}\cos(\omega_1 t + ky)$$

$$\frac{dp_2}{dt} = \sqrt{\alpha\omega_2}\cos(\omega_2 t + ky)$$

$$\frac{dp_3}{dt} = \sqrt{\alpha\omega_3}\cos(\omega_3 t + ky)$$

$$\vdots$$

$$\frac{dp_m}{dt} = \sqrt{\alpha\omega_m}\cos(\omega_m t + ky)$$

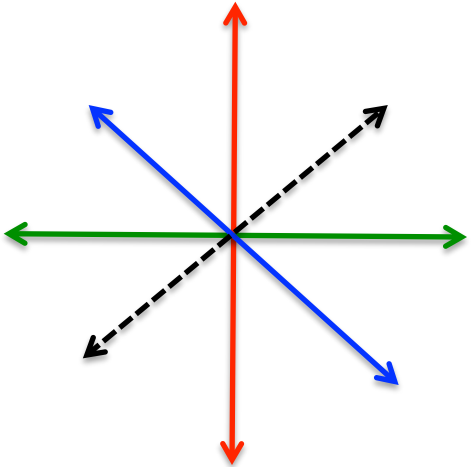

$$\frac{d\mathbf{p}}{dt} = -\frac{k\alpha}{2}\left(\nabla_{\mathbf{p}} V(\mathbf{x}, t)\right)^T$$

On average, the system performs minimizes the **unknown, time-varying** function V(x,t)

Allows simultaneous tuning of ALL parameters in parallel.

$$\omega_i = \omega r_i, \;\; r_i \neq r_j \implies \text{ for any } t > 0$$

$$\lim_{\omega \to \infty} \langle \cos(\omega_i t), \cos(\omega_j t) \rangle = \lim_{\omega \to \infty} \int_0^t \cos(\omega_i \tau)\cos(\omega_j \tau) d\tau = 0$$

Bounded Extremum Seeking: Model-Independent Tuning and Optimization

$$\begin{bmatrix} \dot{x}_1 \\ \vdots \\ \dot{x}_n \end{bmatrix} = \dot{\mathbf{x}} = \mathbf{f}(\mathbf{x}, \mathbf{p}, t) = \begin{bmatrix} f_1(x_1, \ldots, x_n, p_1, \ldots, p_m, t) \\ \vdots \\ f_n(x_1, \ldots, x_n, p_1, \ldots, p_m, t) \end{bmatrix}$$

$$y = V(\mathbf{x}, t) + n(t)$$

noise

$$y = (I(t) - I_0)^2 + n(t)$$

Surviving beam current at end.

$$p_1(t) = Q_1 \text{ current}$$
$$\vdots$$
$$p_m(t) = Q_m \text{ current}$$

$$x_1(t) = X_{\text{rms}}(\text{position } 1)$$
$$x_2(t) = Y_{\text{rms}}(\text{position } 1)$$
$$\vdots$$
$$x_n(t) = X_{\text{rms}}(\text{position n})$$

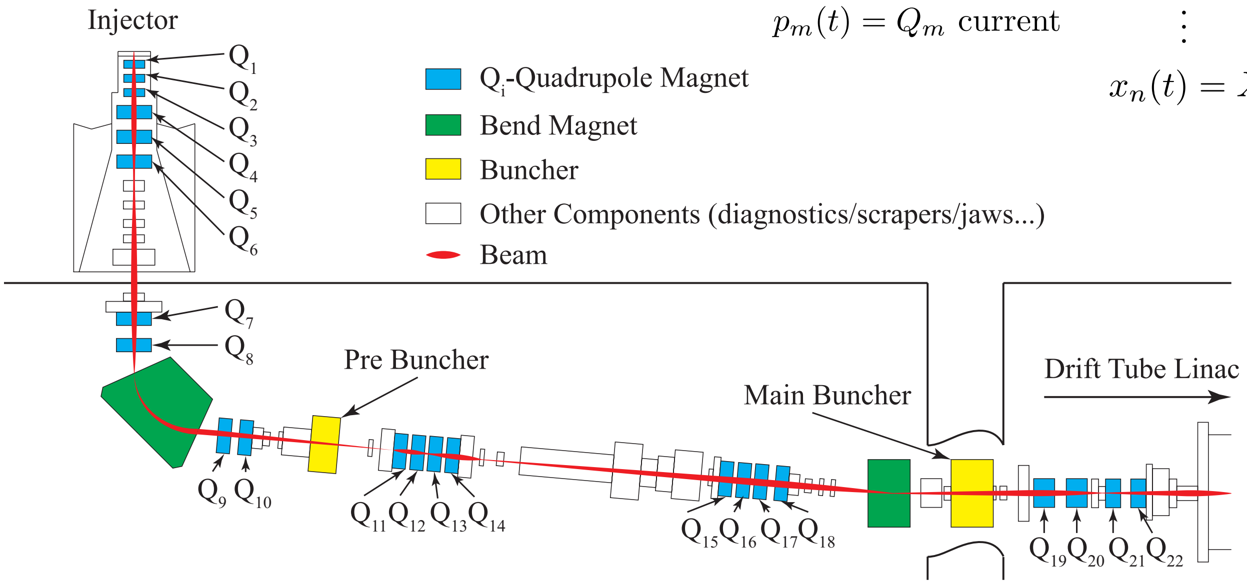

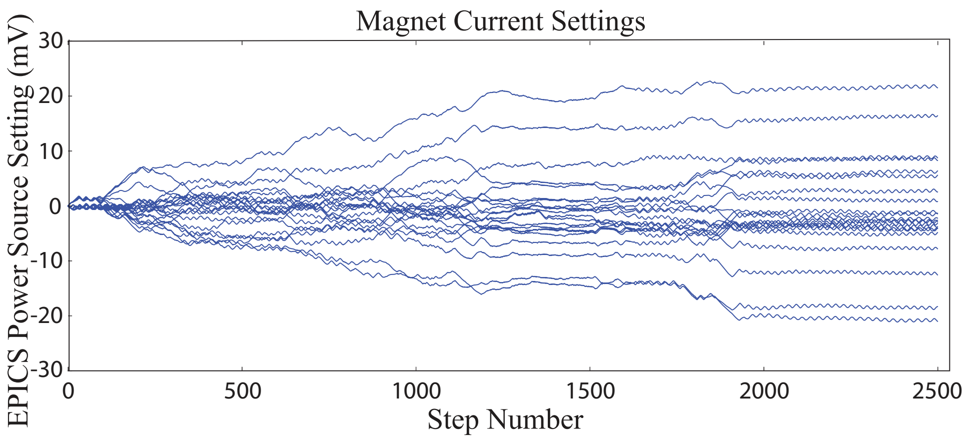

Magnet Current Settings
EPICS Power Source Setting (mV)
30
20
10
0
-10
-20
-30
0
500
1000
1500
2000
2500
Step Number

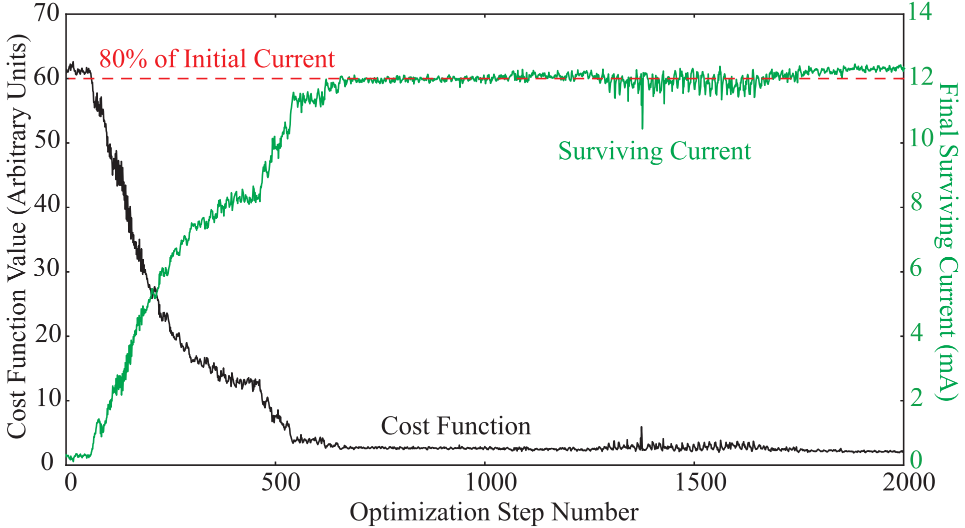

80% of Initial Current
Surviving Current
Cost Function
Cost Function Value (Arbitrary Units)
70
60
50
40
30
20
10
0
Final Surviving Current (mA)
14
12
10
8
6
4
2
0
0
500
1000
1500
2000
Optimization Step Number

$$\dot{x} = x + 0.5y + u_x$$
$$\dot{y} = 0.75x + 2y + u_y$$
$$h = x^2 + y^2$$

$$u_{1,x} = \cos(\omega t + kh(x,y))\sqrt{\alpha\omega}$$

$$u_{1,y} = \sin(\omega t + kh(x,y))\sqrt{\alpha\omega}$$

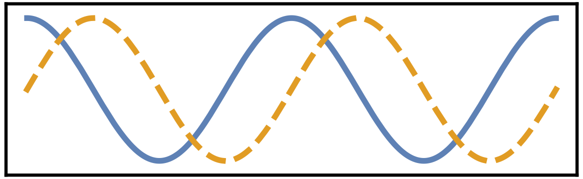

$$\dot{x} = x + 0.5y + u_x$$
$$\dot{y} = 0.75x + 2y + u_y$$
$$h = x^2 + y^2$$

$$u_{1,x} = \cos(\omega t + kh(x,y))\sqrt{\alpha\omega} \qquad u_{1,y} = \sin(\omega t + kh(x,y))\sqrt{\alpha\omega}$$

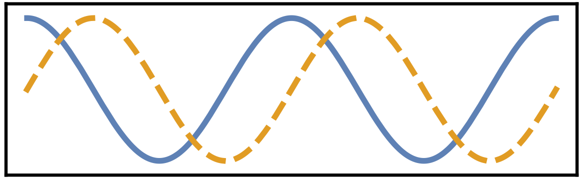

$$u_{2,x} = f_{\mathrm{tri},1}(\omega t + kh(x,y))\frac{4}{\pi}\sqrt{\alpha\omega} \qquad u_{2,y} = f_{\mathrm{tri},2}(\omega t + kh(x,y))\frac{4}{\pi}\sqrt{\alpha\omega}$$

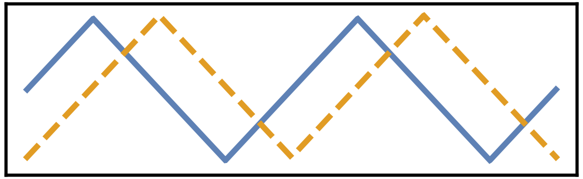

$$\dot{x} = x + 0.5y + u_x$$
$$\dot{y} = 0.75x + 2y + u_y$$
$$h = x^2 + y^2$$

$$u_{1,x} = \cos(\omega t + kh(x,y))\sqrt{\alpha\omega} \qquad u_{1,y} = \sin(\omega t + kh(x,y))\sqrt{\alpha\omega}$$

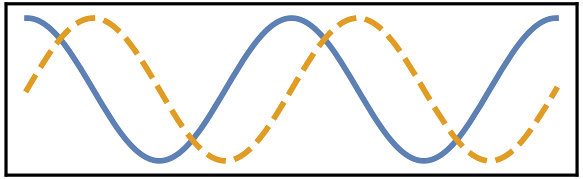

$$u_{2,x} = f_{\mathrm{tri},1}(\omega t + kh(x,y))\frac{4}{\pi}\sqrt{\alpha\omega} \qquad u_{2,y} = f_{\mathrm{tri},2}(\omega t + kh(x,y))\frac{4}{\pi}\sqrt{\alpha\omega}$$

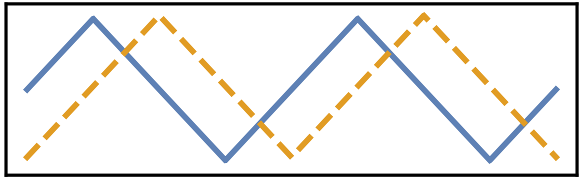

$$u_{3,x} = f_{\mathrm{sqr},1}(\omega t + kh(x,y))\frac{2}{\pi}\sqrt{\alpha\omega} \qquad u_{3,y} = f_{\mathrm{sqr},2}(\omega t + kh(x,y))\frac{2}{\pi}\sqrt{\alpha\omega}$$

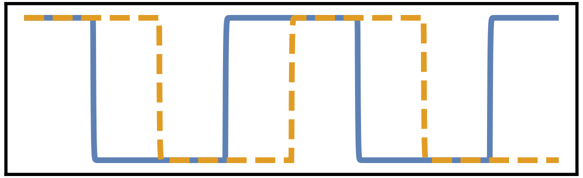

$$\dot{x} = x + 0.5y + u_x$$
$$\dot{y} = 0.75x + 2y + u_y$$
$$h = x^2 + y^2$$

$$u_{1,x} = \cos(\omega t + kh(x,y))\sqrt{\alpha\omega} \qquad u_{1,y} = \sin(\omega t + kh(x,y))\sqrt{\alpha\omega}$$

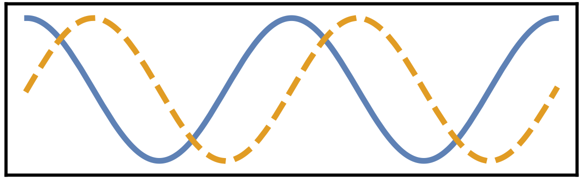

$$u_{2,x} = f_{\mathrm{tri},1}(\omega t + kh(x,y))\frac{4}{\pi}\sqrt{\alpha\omega} \qquad u_{2,y} = f_{\mathrm{tri},2}(\omega t + kh(x,y))\frac{4}{\pi}\sqrt{\alpha\omega}$$

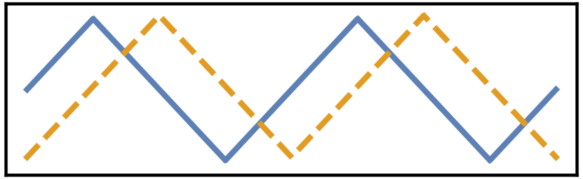

$$u_{3,x} = f_{\mathrm{sqr},1}(\omega t + kh(x,y))\frac{2}{\pi}\sqrt{\alpha\omega} \qquad u_{3,y} = f_{\mathrm{sqr},2}(\omega t + kh(x,y))\frac{2}{\pi}\sqrt{\alpha\omega}$$

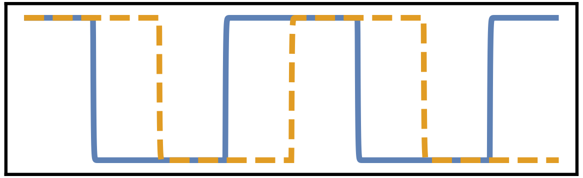

$$u_{4,x} = f_{\mathrm{sqrd},1}(\omega t + kh(x,y))\frac{2}{\pi}\sqrt{\alpha\omega} \qquad u_{4,y} = f_{\mathrm{sqrd},2}(\omega t + kh(x,y))\frac{2}{\pi}\sqrt{\alpha\omega}$$

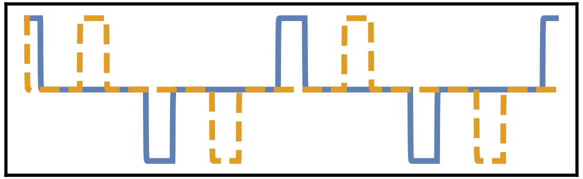

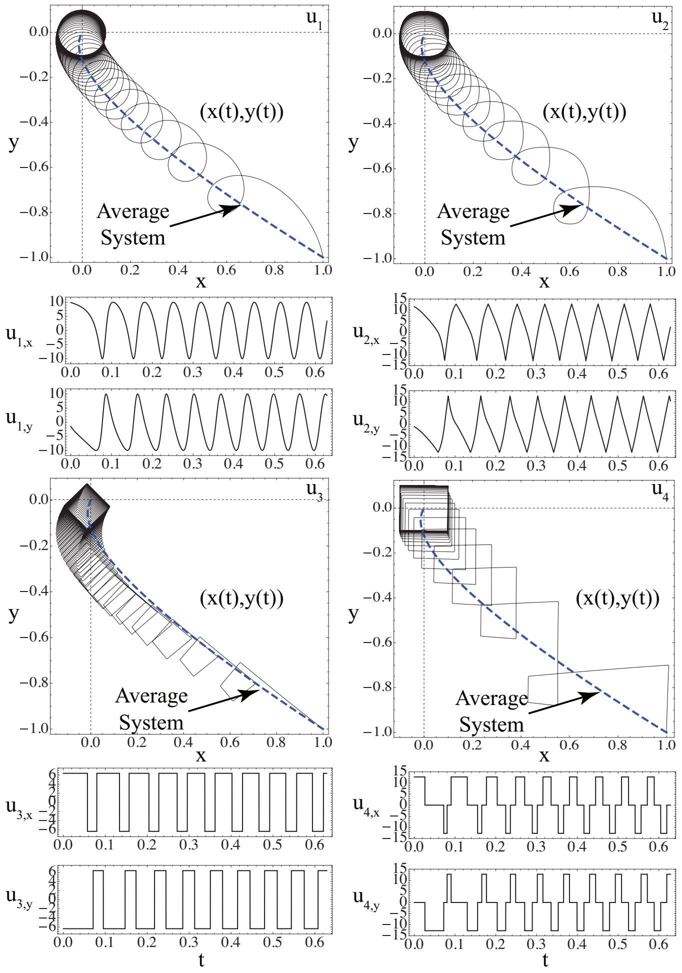

u1
(x(t),y(t))
Average System
y
x
u1,x
u1,y
u2
(x(t),y(t))
Average System
u2,x
u2,y
u3
(x(t),y(t))
Average System
u3,x
u3,y
u4
(x(t),y(t))
Average System
u4,x
u4,y
t

Cost is noisy measurement of the difference between initial current into the machine and surviving current at the end of the transport region.

$$y = (I(t) - I_0)^2 + n(t)$$

Minimization of y equivalent to properly tuning magnets for all beam to be transported.

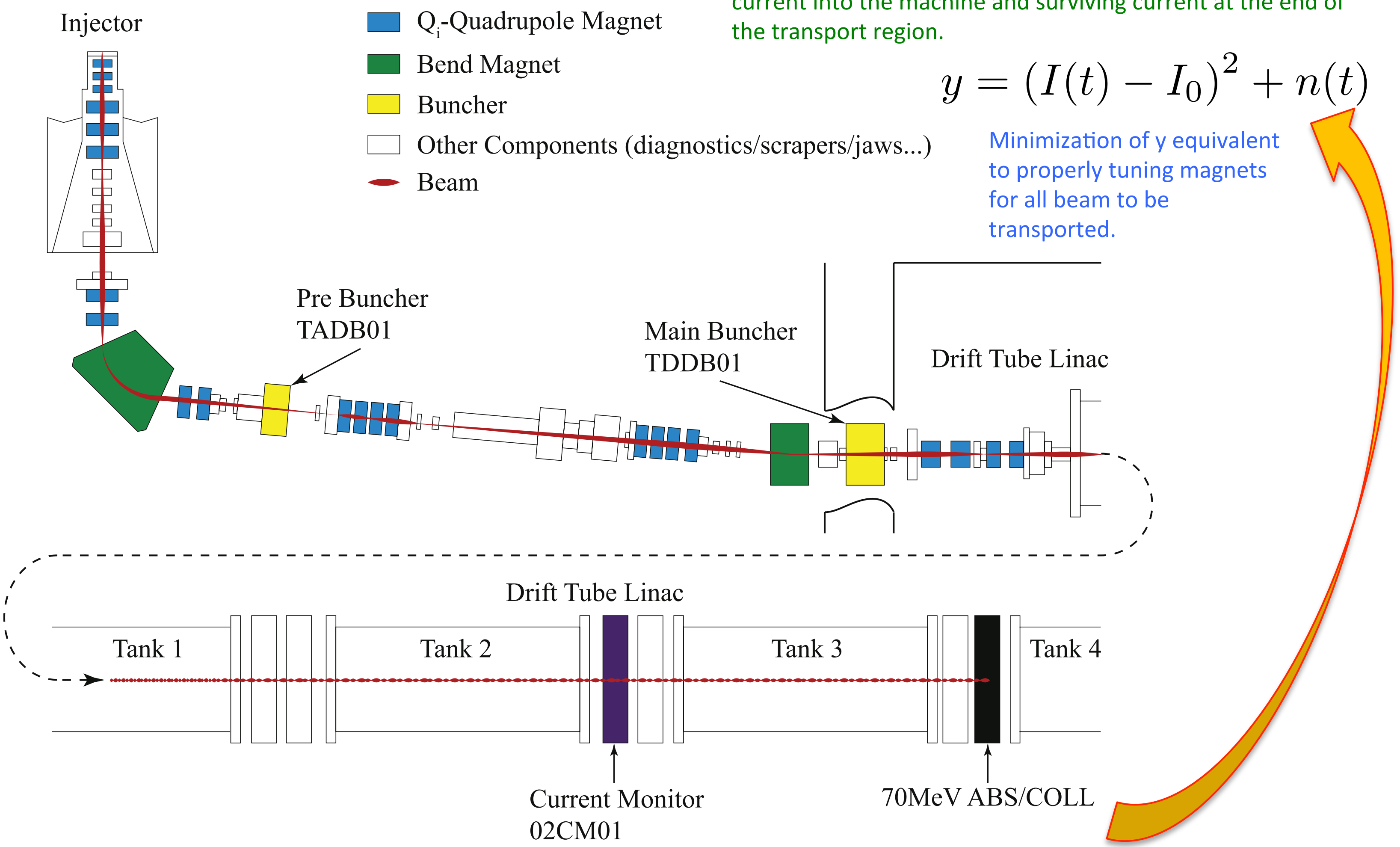

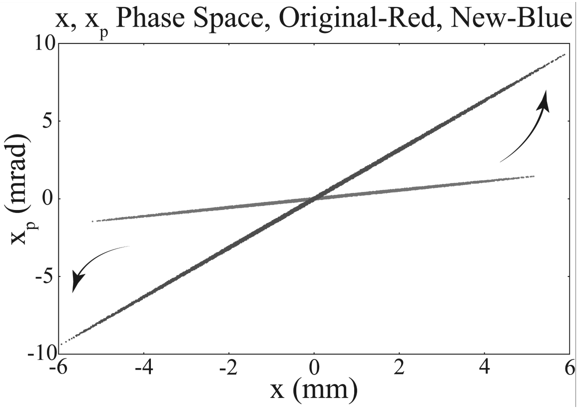

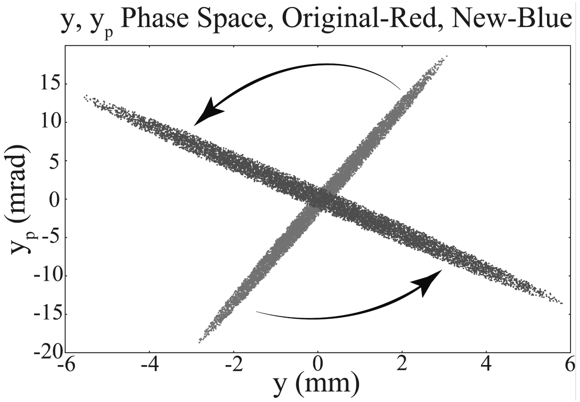

After the magnetic lattice was matched to transport the beam, beam phase space was continuously varied, and arbitrary phase drifts were introduced into the RF buncher cavities.

Without adaptive feedback all beam is quickly lost (red line in figure below).

With adaptive tuning the 22 quad magnetic lattice and 2 RF buncher cavities are continuously re-tuned to maintain maximal beam transmission and acceleration.

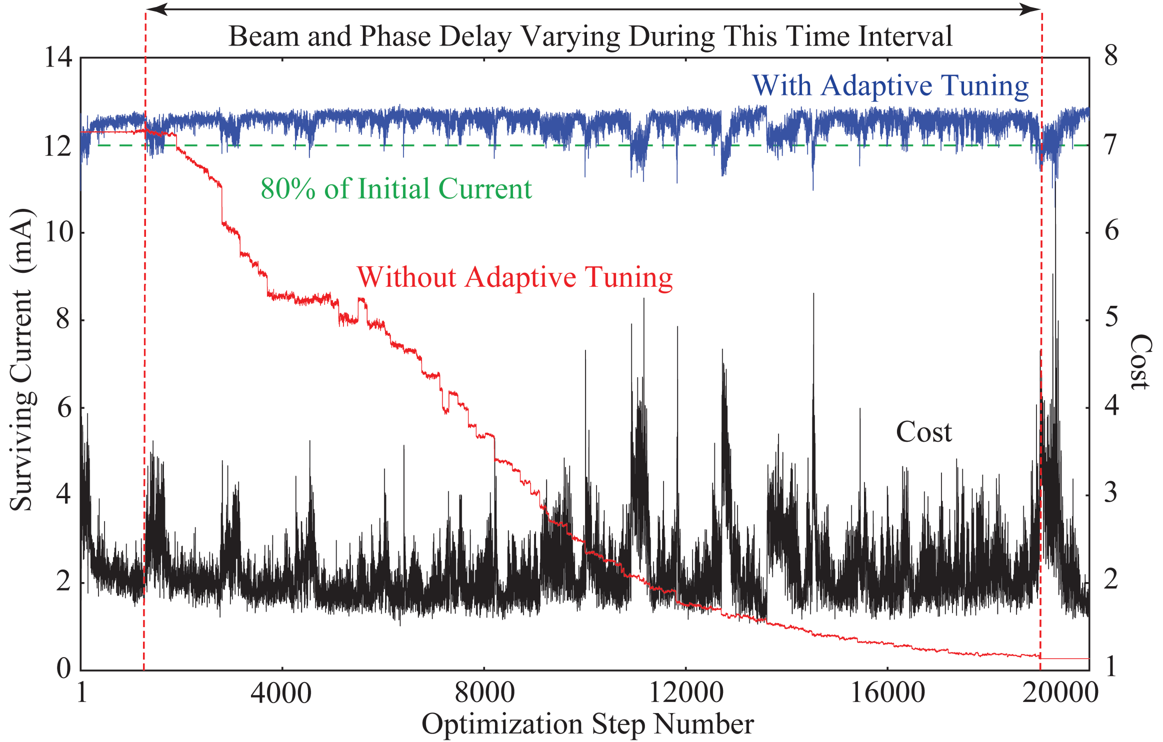

A. Scheinker et al., “Minimization of Betatron oscillations of electron beam injected into a time-varying lattice via extremum seeking,” *IEEE Transactions on Control Systems Technology*, 2016.

SPEAR3 time-varying magnetic lattice

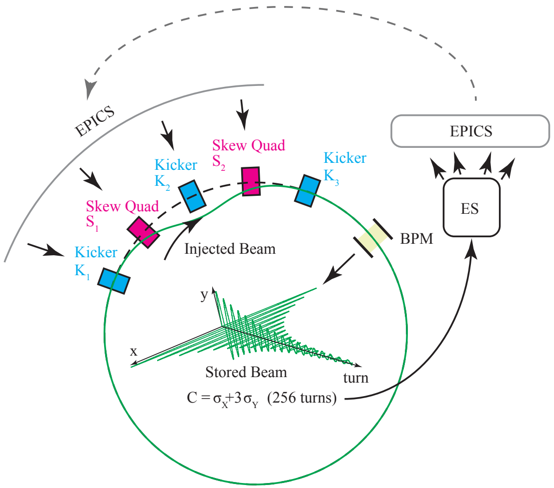

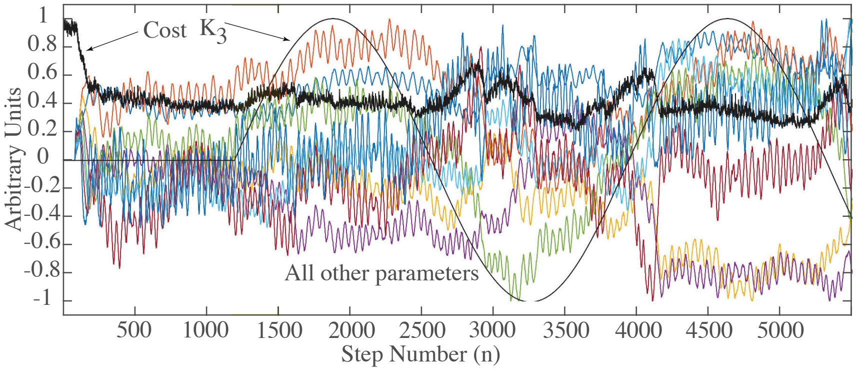

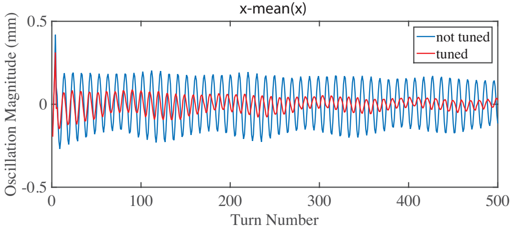

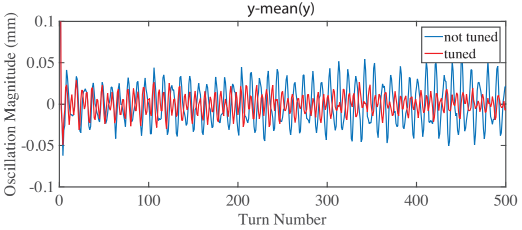

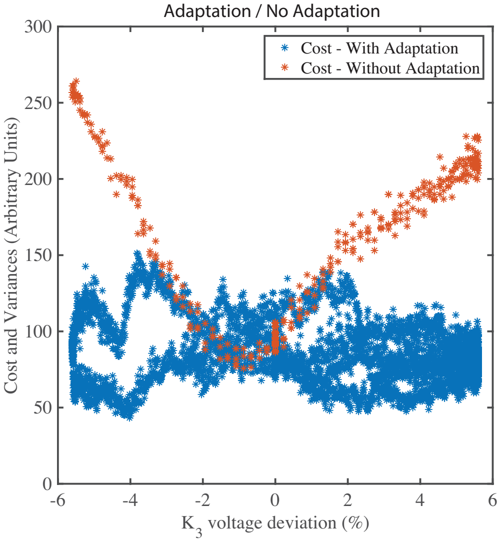

A. Scheinker. "Iterative Extremum Seeking for Feedforward Compensation of Beam Loading in Particle Accelerator RF Cavities ," in *Proceedings of the 2017 American Control Conference*, May, 2017.

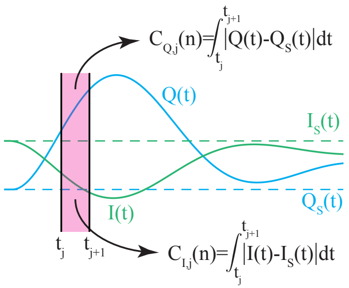

Break up cavity field errors into slices and create costs for iterative minimization

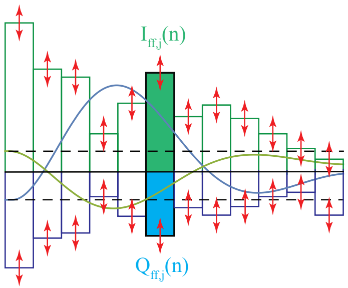

Create feed-forward waveforms for each slice to compensate for beam loading

H+ 21mA peak current, 625μs pulses

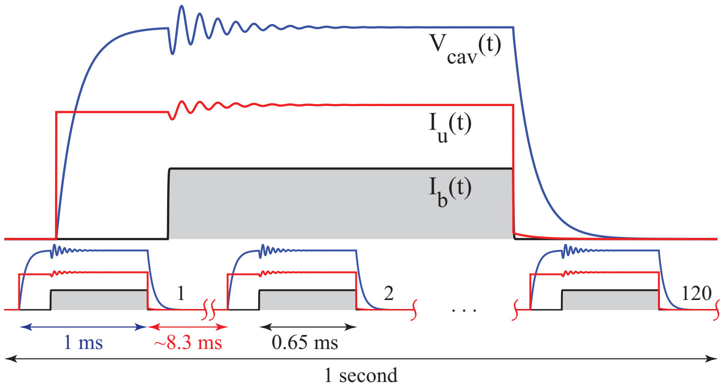

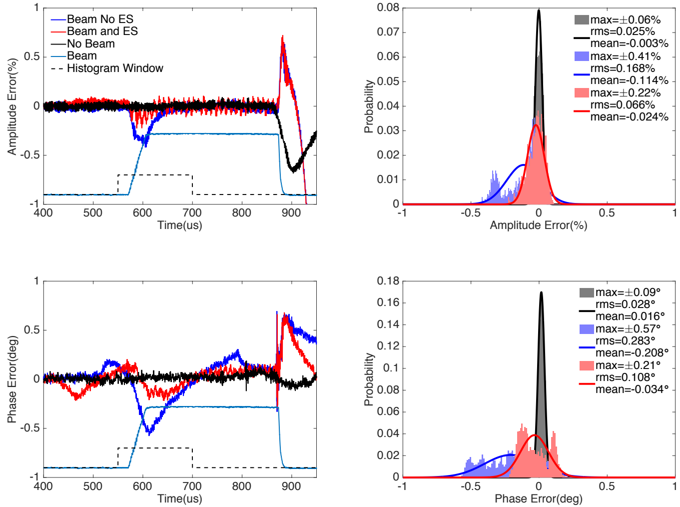

FACET: E-bunch profile prediction based on non-destructive measurements of energy spread spectrum. A. Scheinker and S. Gessner, "Adaptive method for electron bunch profile prediction," *Physical Review Accelerators and Beams*, 18, 102801, 2015.

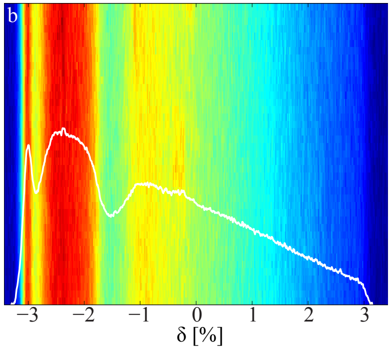

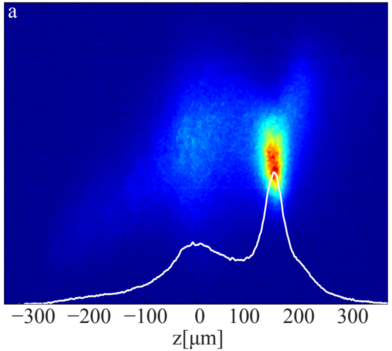

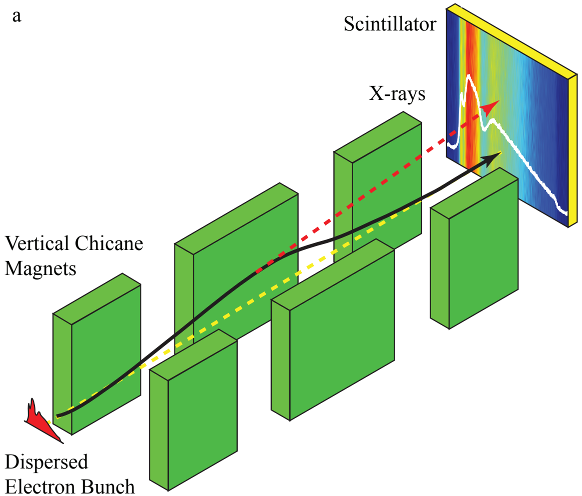

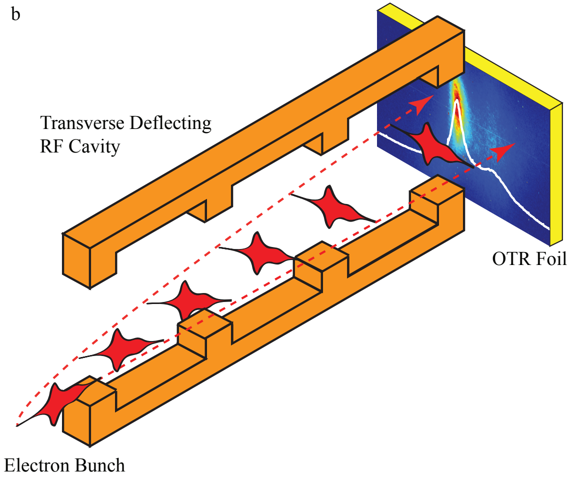

FACET: E-bunch profile prediction based on non-destructive measurements of energy spread spectrum. A. Scheinker and S. Gessner, "Adaptive method for electron bunch profile prediction," *Physical Review Accelerators and Beams*, 18, 102801, 2015.

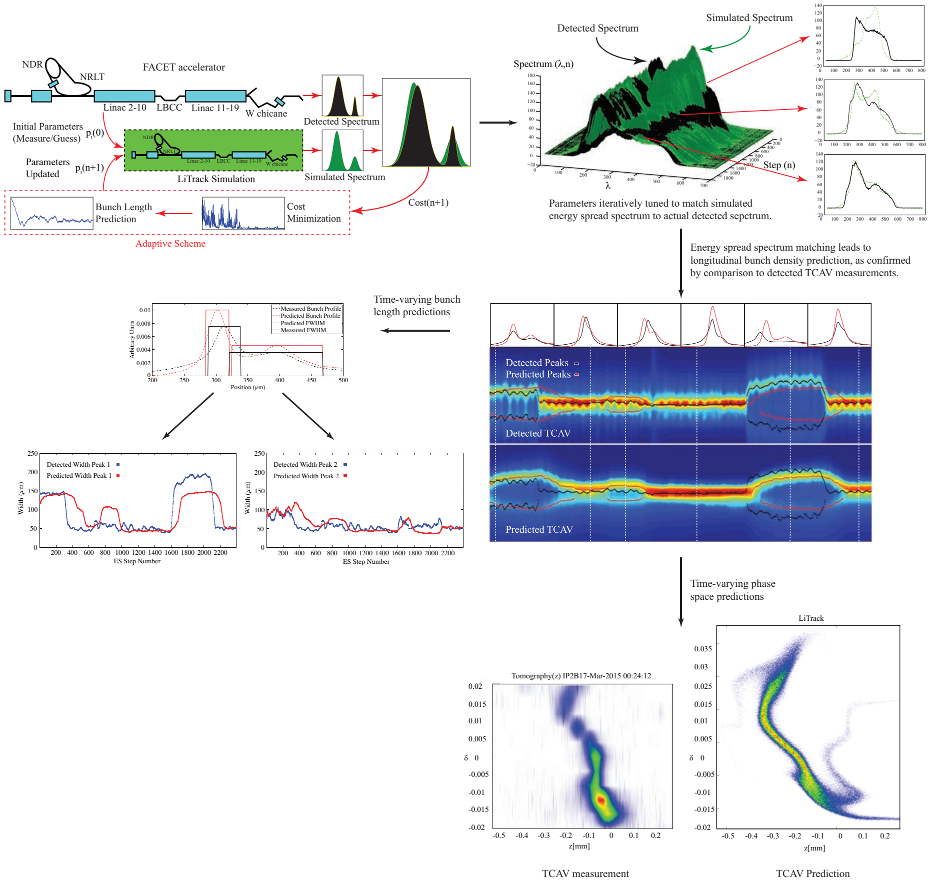

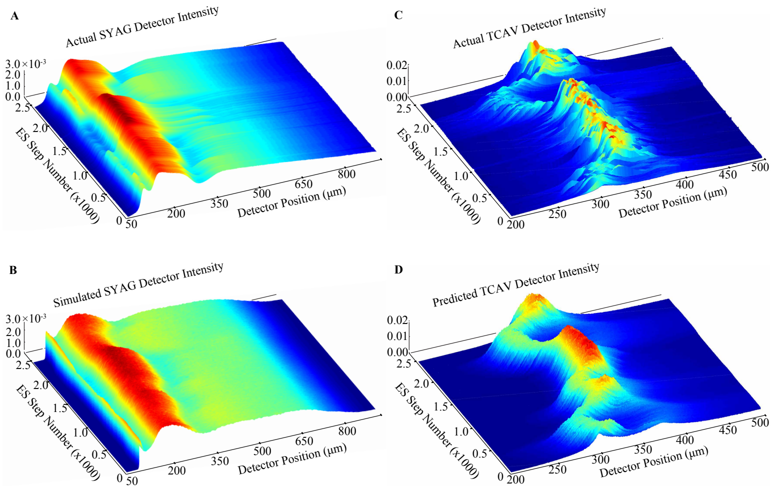

FACET-II Virtual Diagnostics and Phase Space Control: Adjusting RF phases to match energy spread spectrums

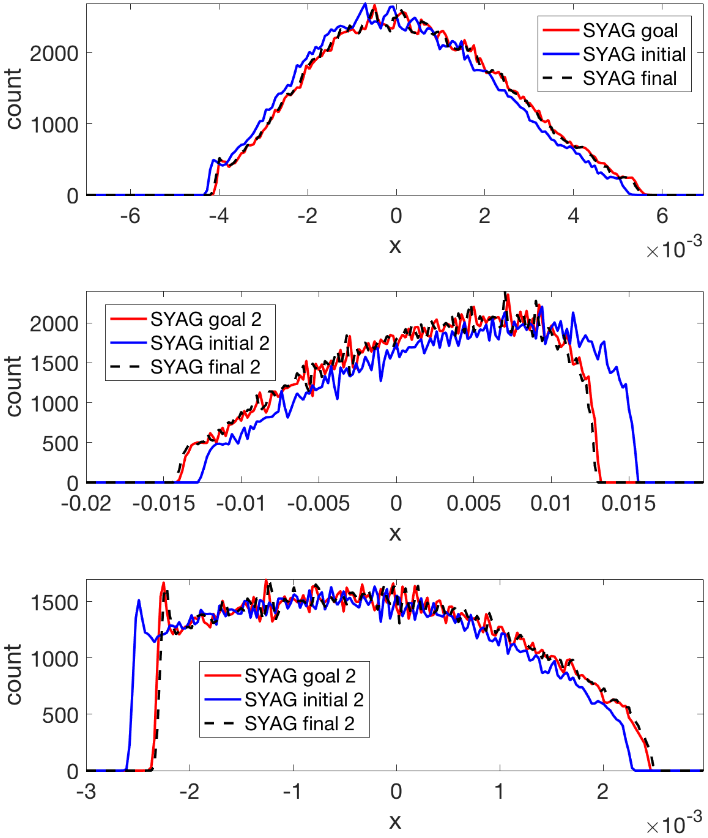

FACET-II Virtual Diagnostics and Phase Space Control: Adjusting RF phases to match energy spread spectrums

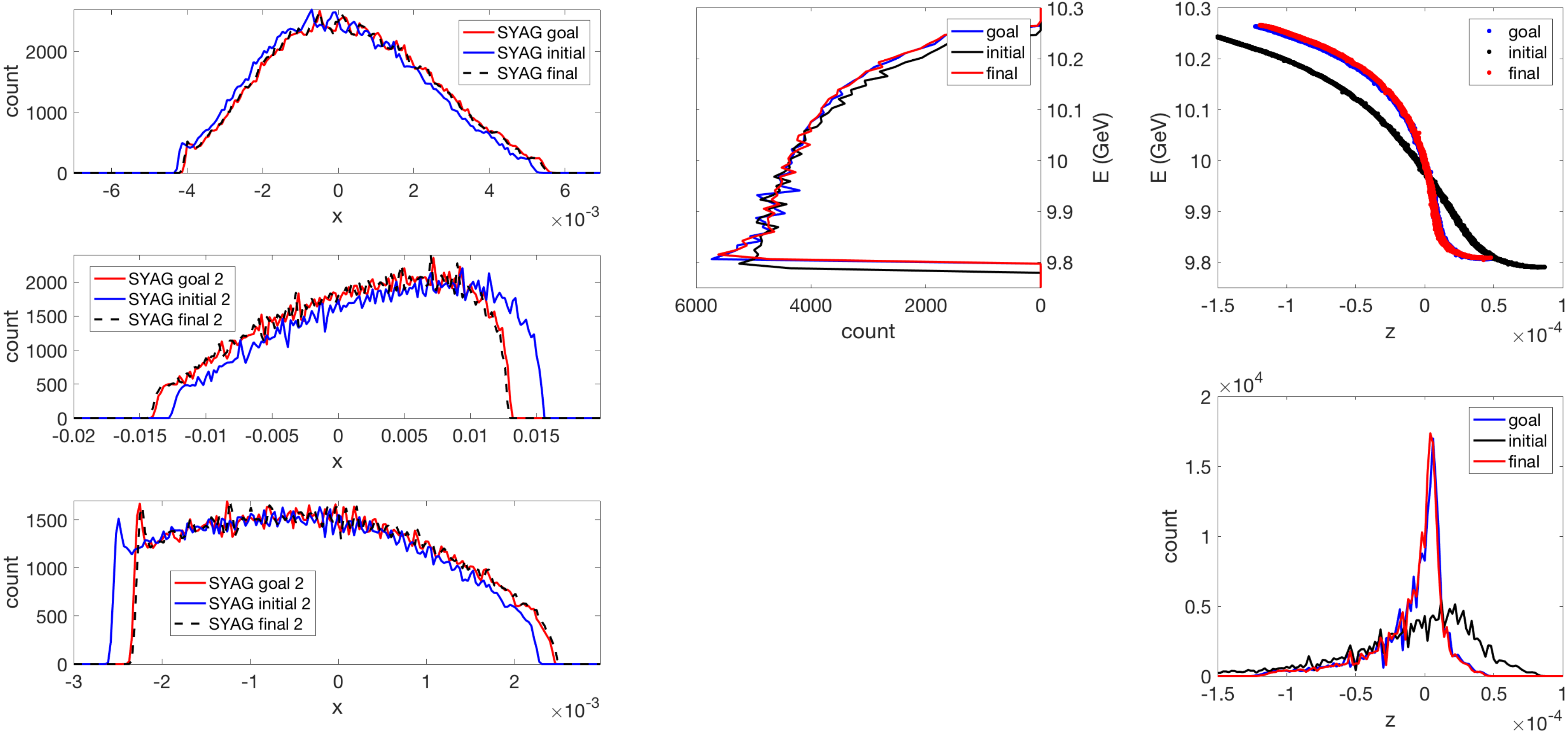

LCLS automatic longitudinal phase space tuning: A. Scheinker et al., "Demonstration of model-independent control of the longitudinal phase space of electron beams in the LCLS with fs resoltuions," *submitted.*

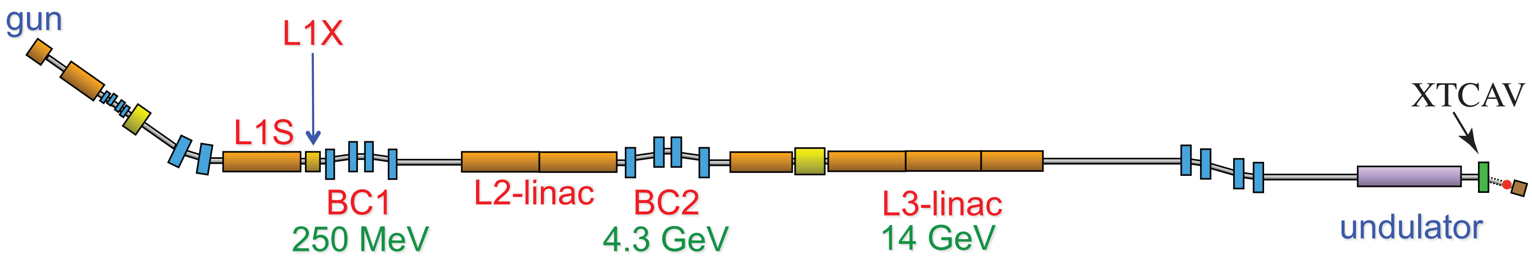

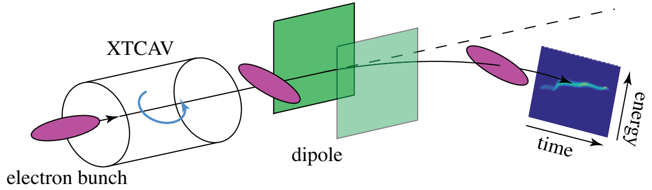

$$\rho_e(E) = \int_{-\Delta L}^{\Delta L} \rho(z,E)dz, \qquad \rho_c(z) = \int_{-\Delta E}^{\Delta E} \rho(z,E)dE$$

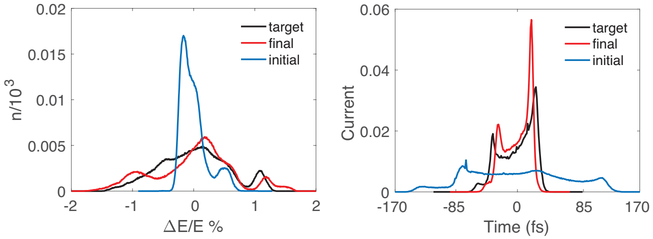

$$C = c_1 \int_{-\Delta L}^{\Delta L} |\hat{\rho}_c(z) - \rho_c(z)|\, dz + c_2 \int_{-\Delta E}^{\Delta E} |\hat{\rho}_e(E) - \rho_e(E)|\, dE$$

LCLS automatic longitudinal phase space tuning. A. Scheinker. and D Bohler, "Demonstration of model-independent control of the longitudinal phase space of electron beams in the LCLS with fs resoltuions," *submitted.*

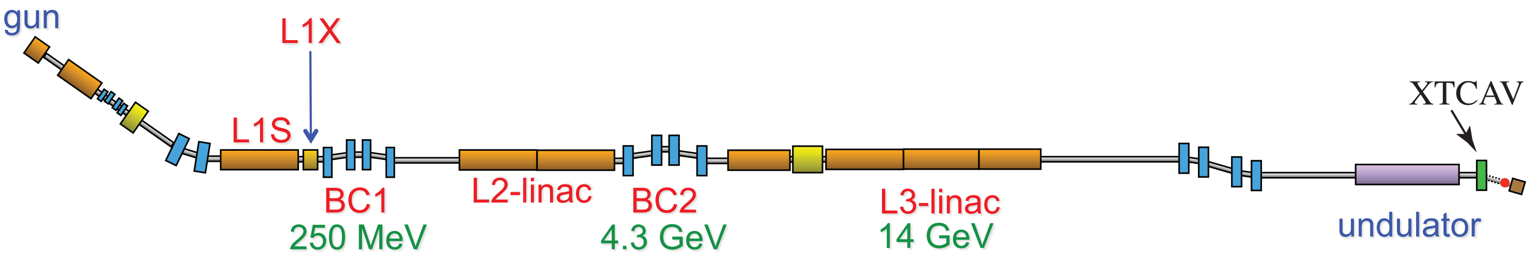

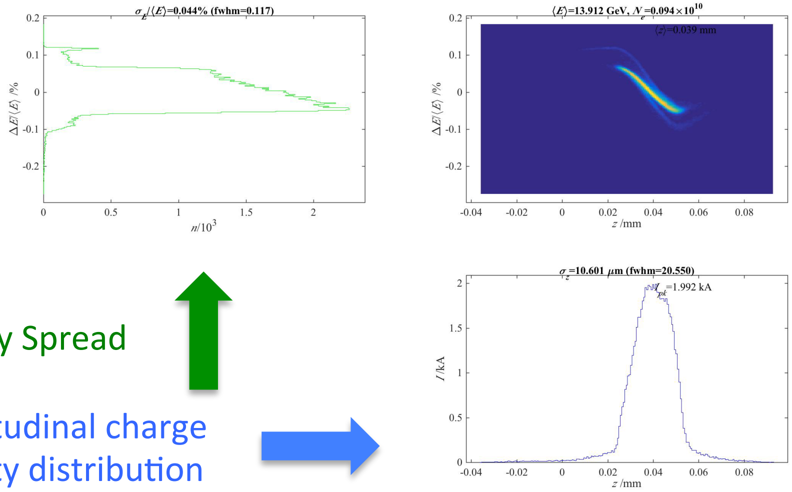

Energy Spread

Longitudinal charge density distribution

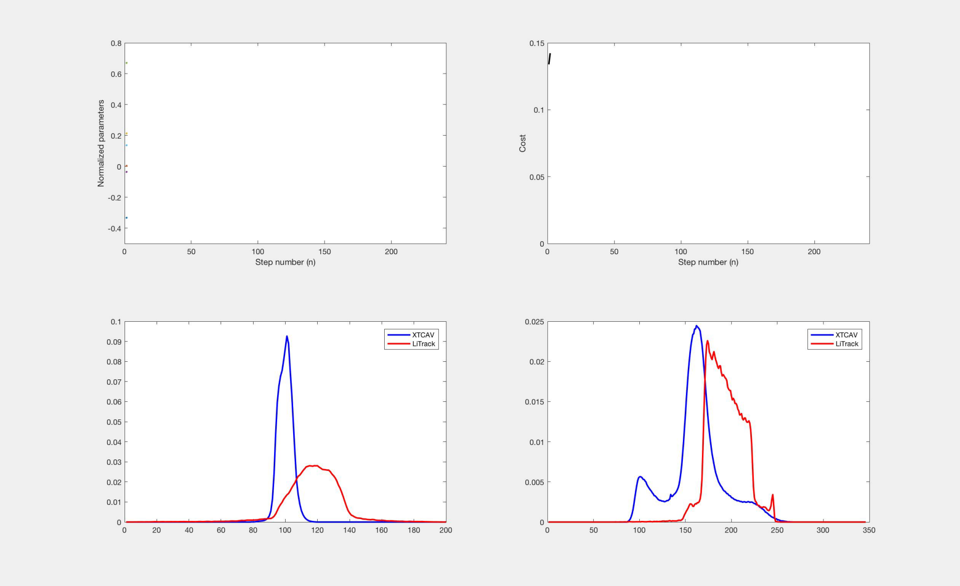

6 parameters being tuned

Normalized within [-1, 1]

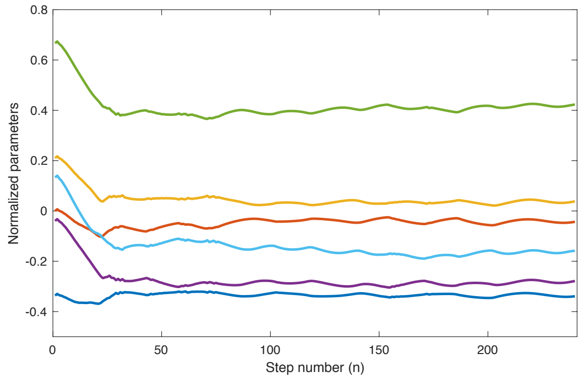

Cost function being minimized

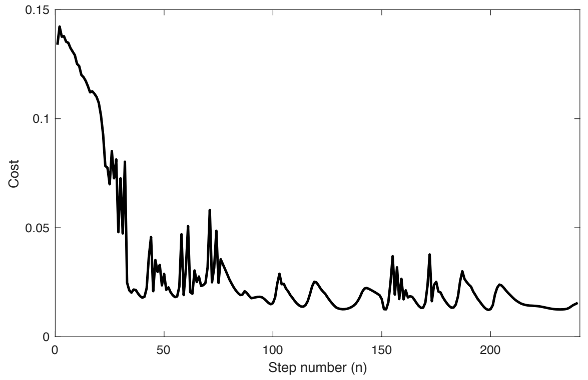

Longitudinal charge density distribution

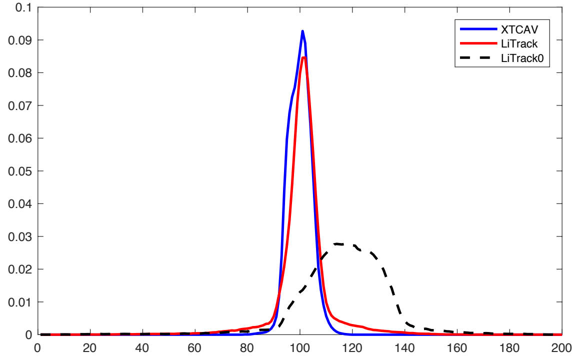

Energy Spread

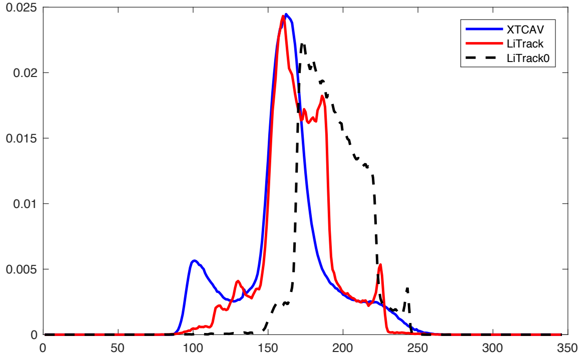

LiTrackES intial

LiTrackES final

Goal

TABLE I. Experiment setup details.

Experiment	Beam energy (GeV)	Bunch charge (nC)	k	α	ω	dt	Averaging	Cost function
1	4.48	0.17	1.0E-3	9	[2000, 2320, 2640, 2960, 3280, 3600]	8.7E-5	10×	1D projections
2	4.48	0.17	1.0E-3	4	[2000, 2320, 2640, 2960, 3280, 3600]	8.7E-5	10×	1D projections
3	13.42	0.18	1.4E-5	10	1000	6.3E-4	none	2D images

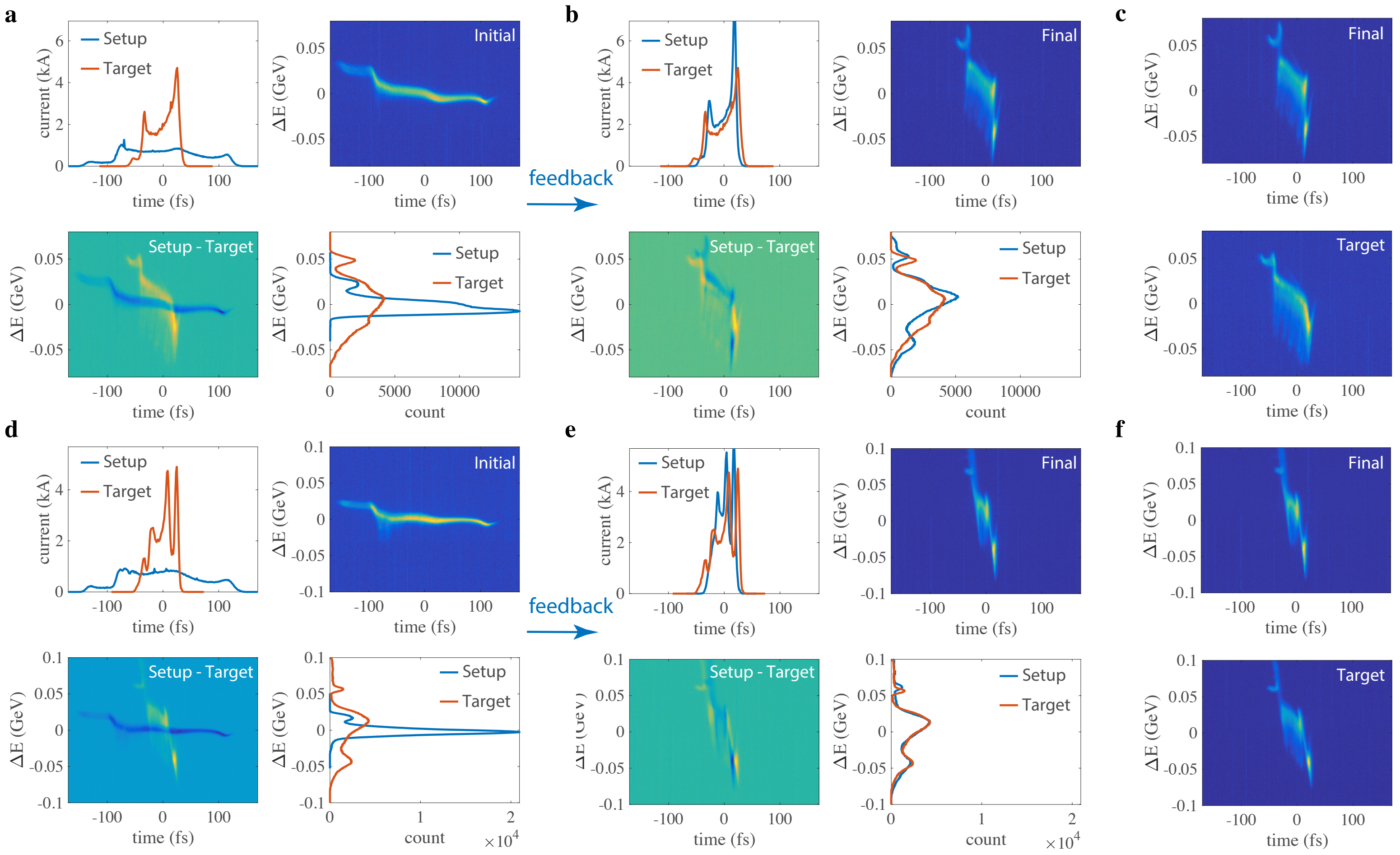
a
b
c
d
e
f
Setup
Target
Initial
Final
Setup - Target
feedback
current (kA)
ΔE (GeV)
time (fs)
count
$\times 10^4$

ES in OCELOT for time-varying systems

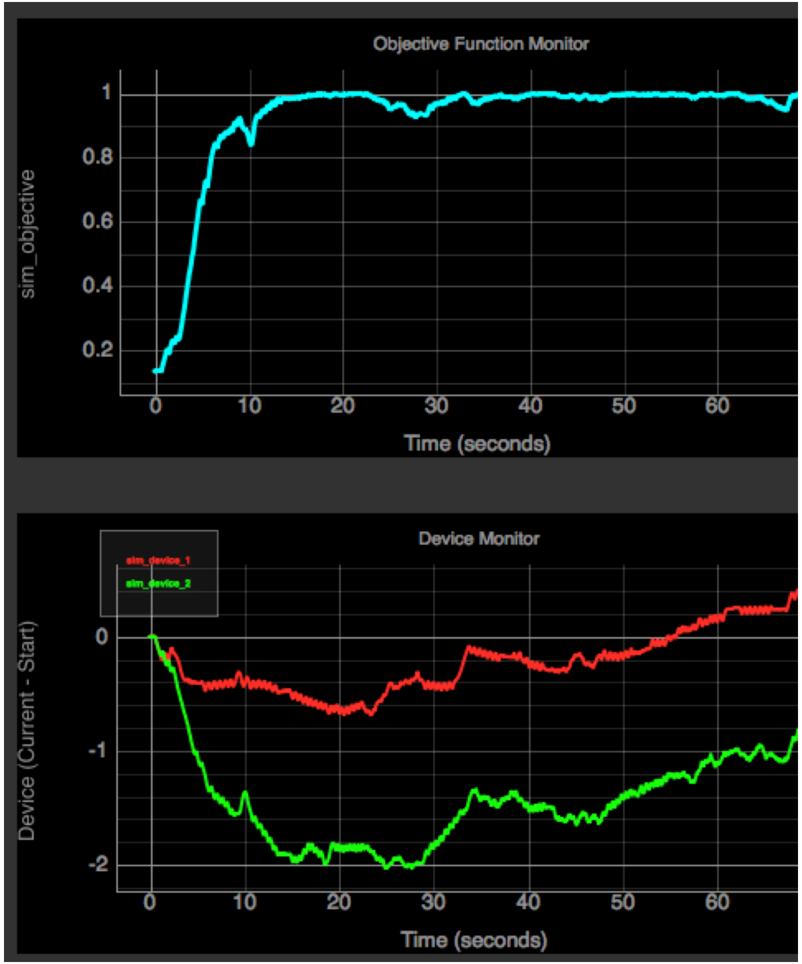

Combining ML and ES

(LANL and SLAC)

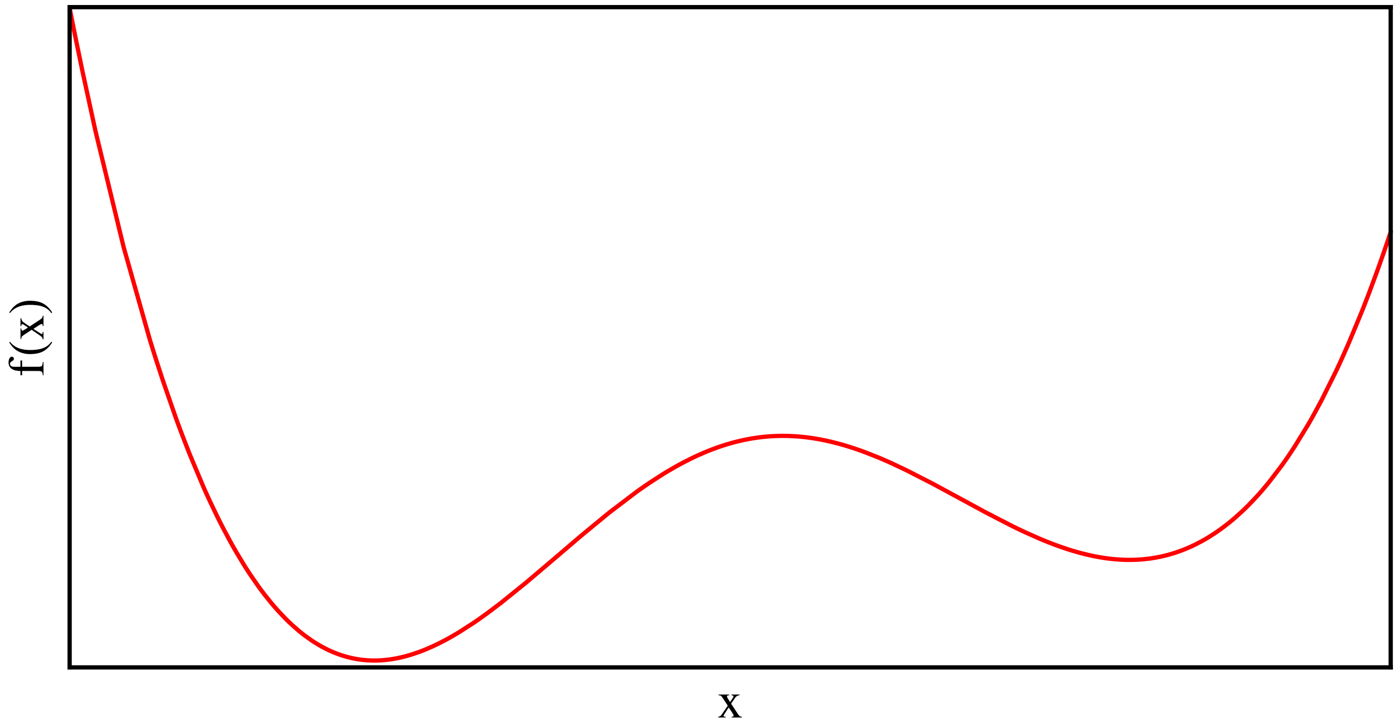
f(x)
x

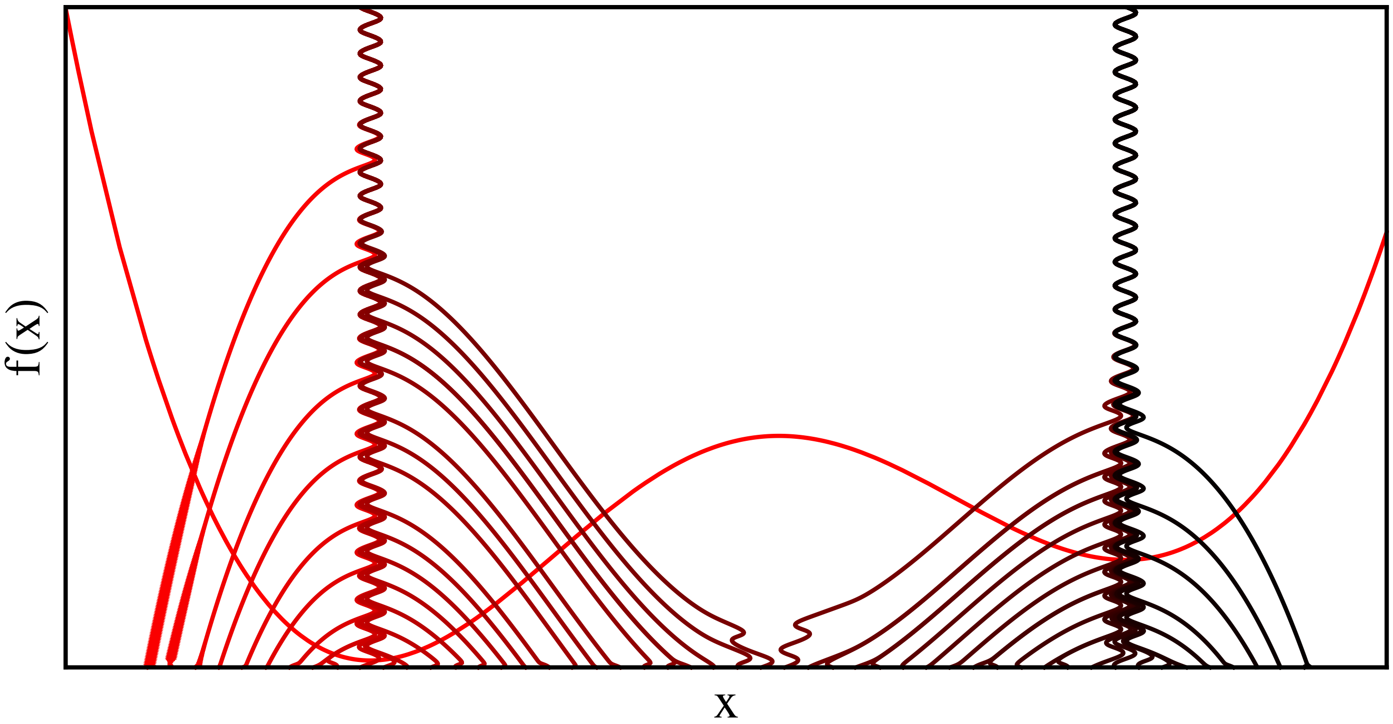
f(x)
x

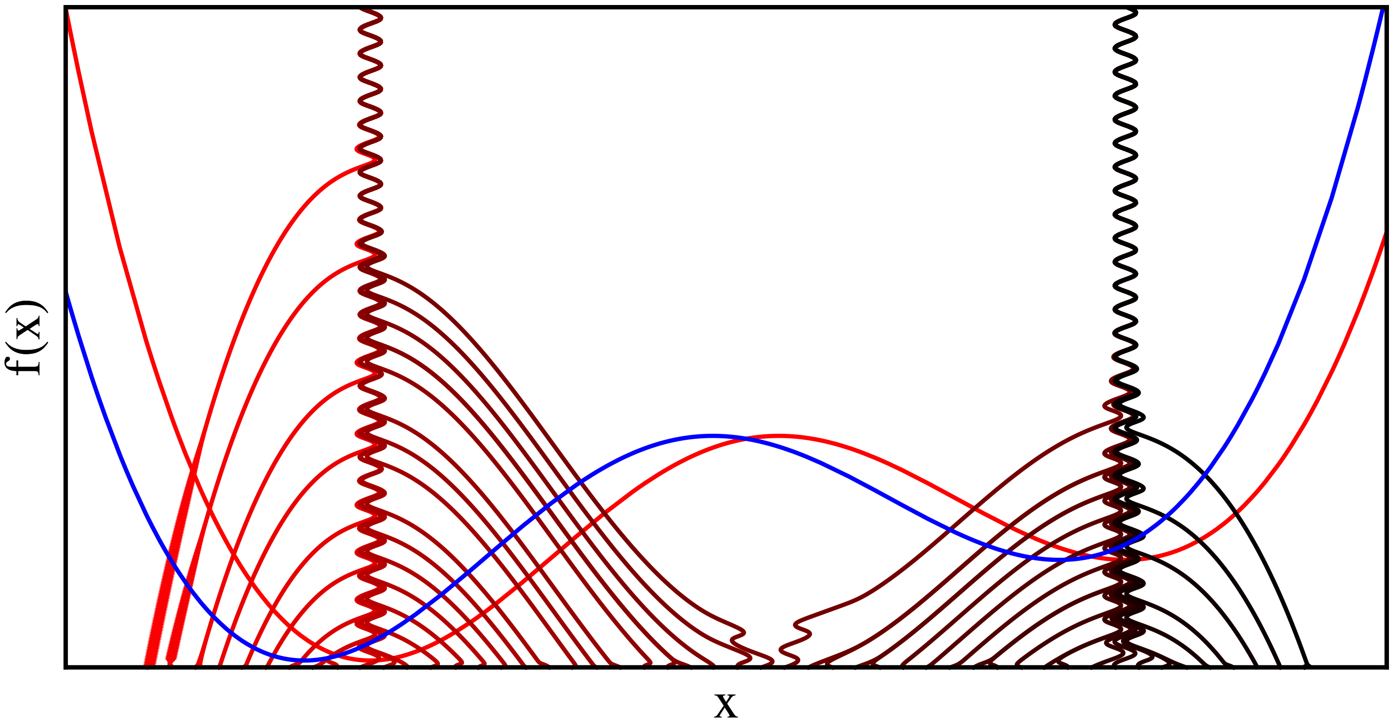

f(x)
x

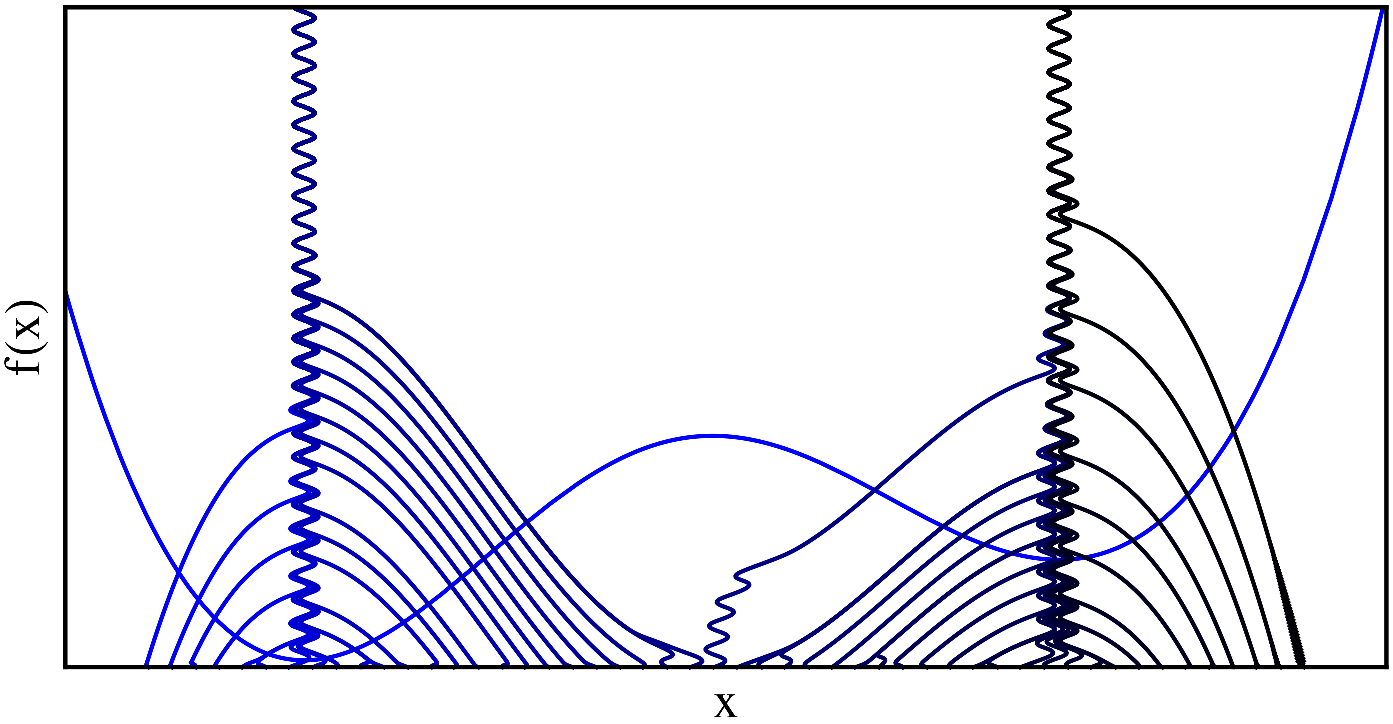
f(x)
x

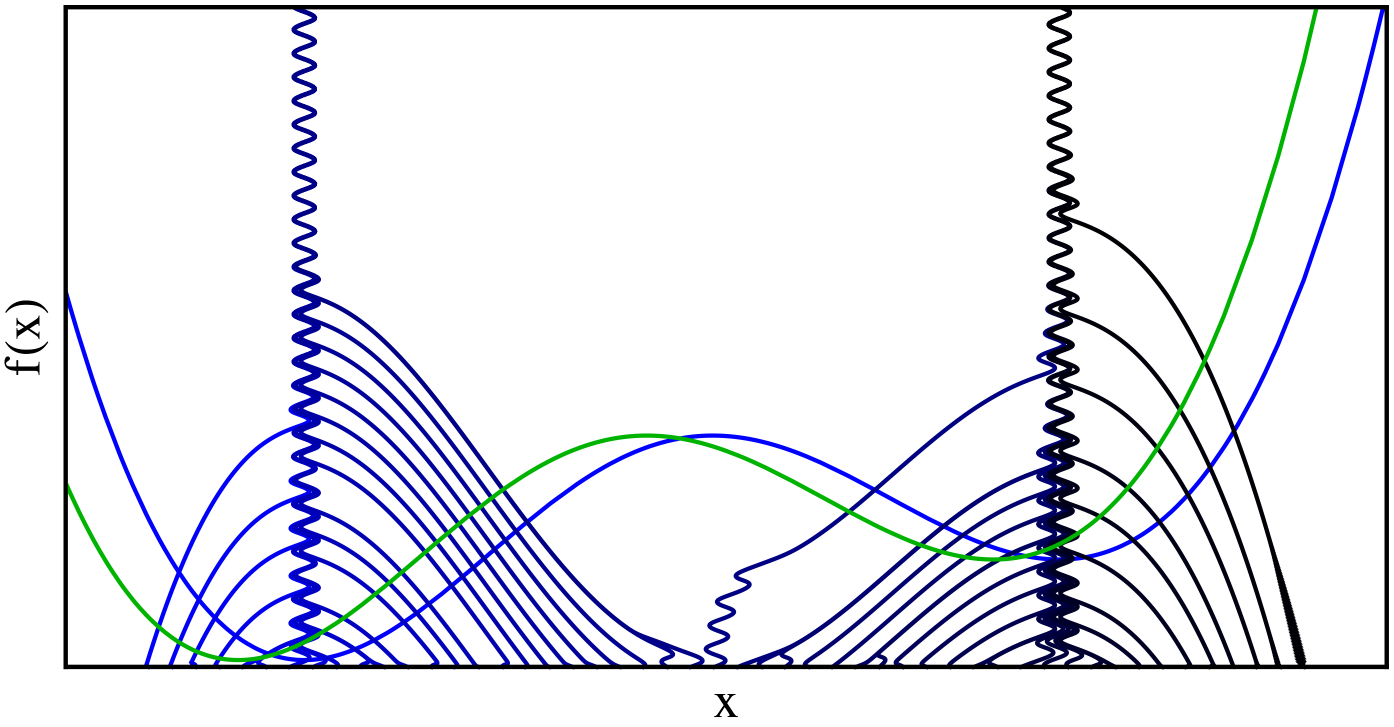
f(x)
x

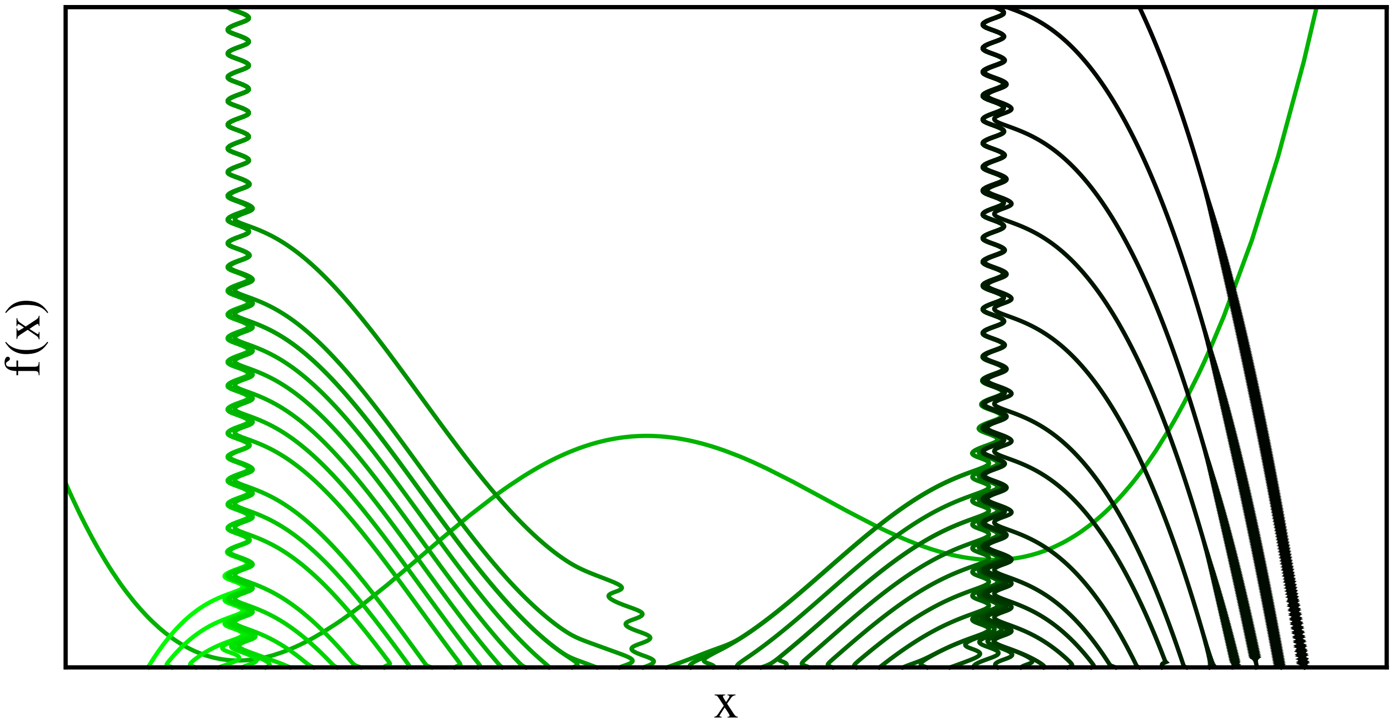
f(x)
x

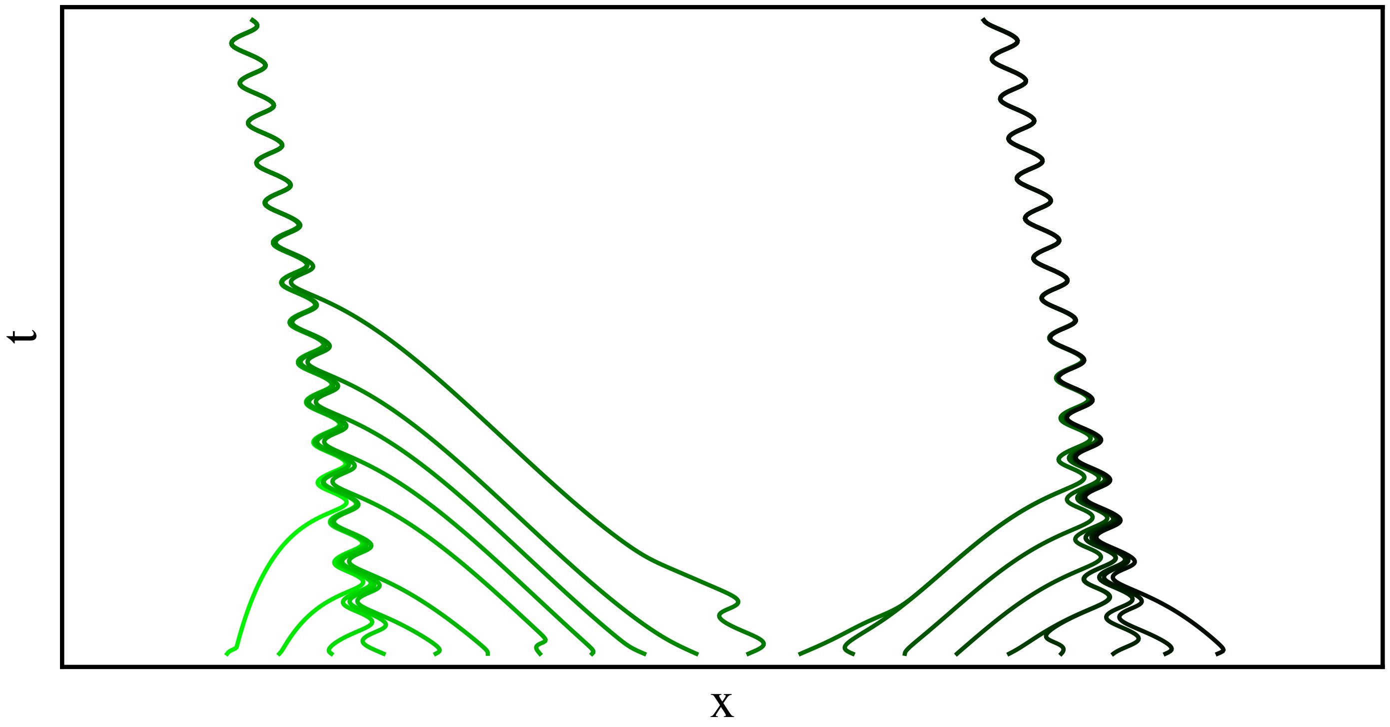
t
x

Re-training a deep NN with many output nodes would take too long

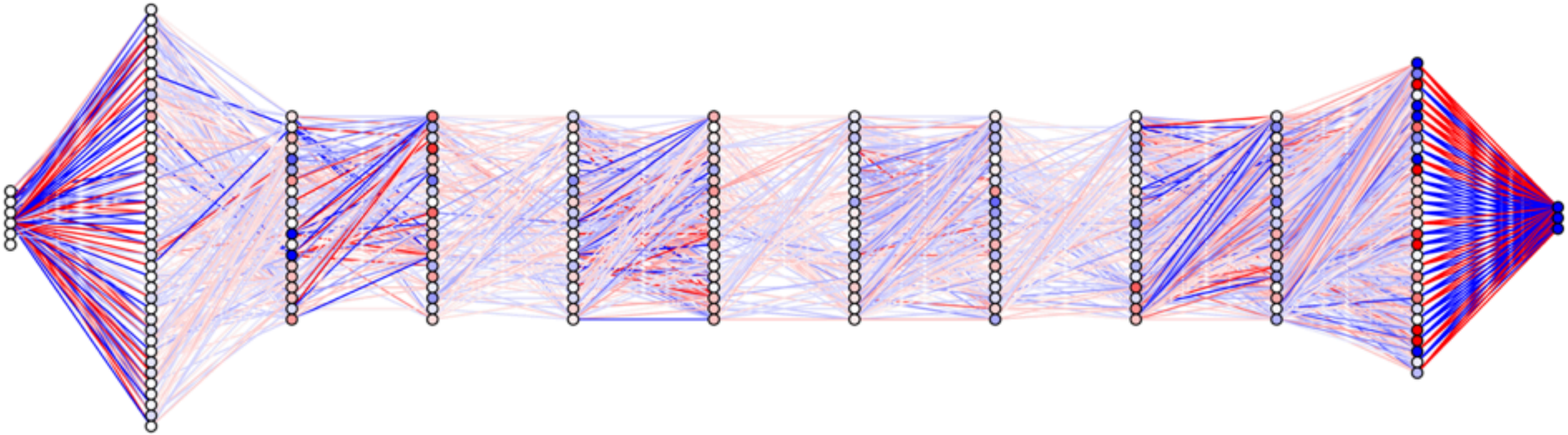

Ongoing work

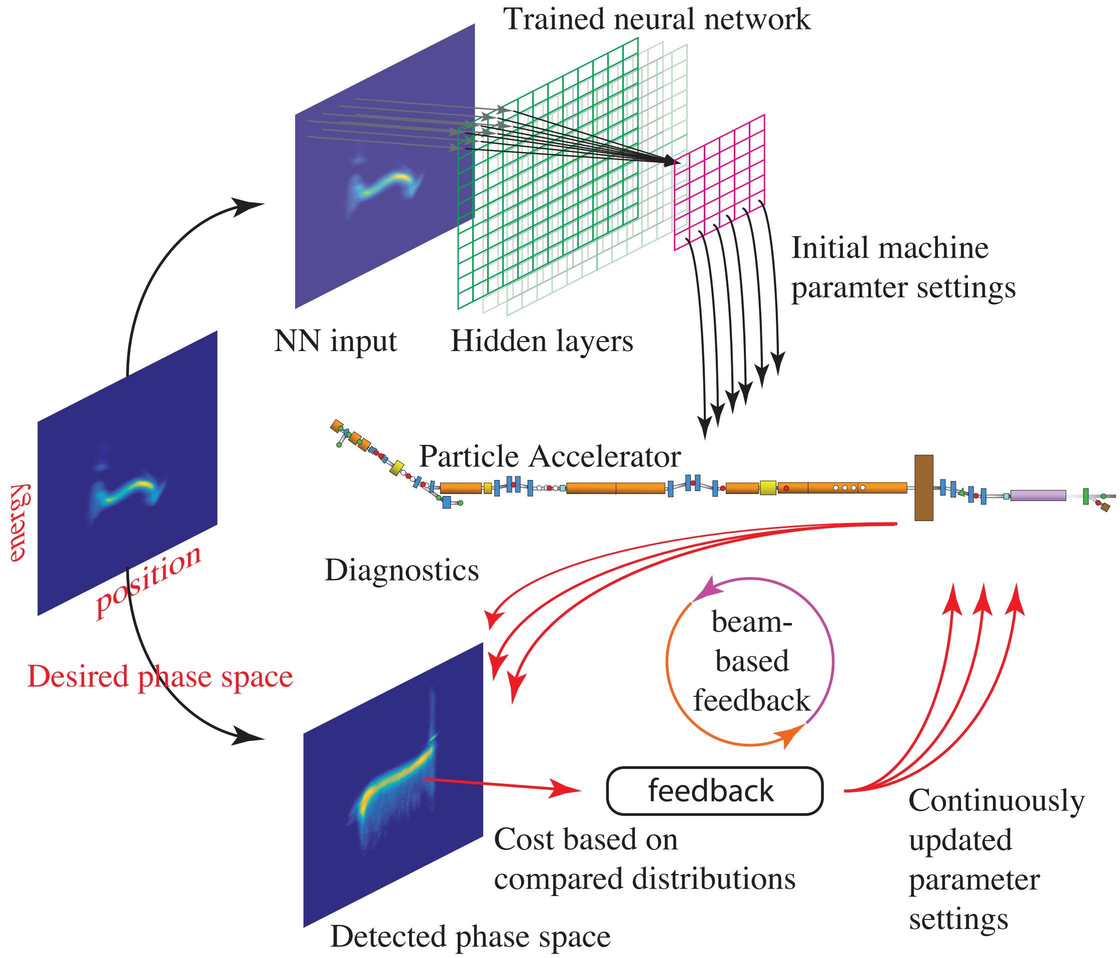

LCLS automatic longitudinal phase space tuning: **Alexander Scheinker, Auralee Edelen, Dorian Bohler, Claudio Emma, and Alberto Lutman,** "Demonstration of model-independent control of the longitudinal phase space of electron beams in the LCLS with fs resoltuions," *submitted.*

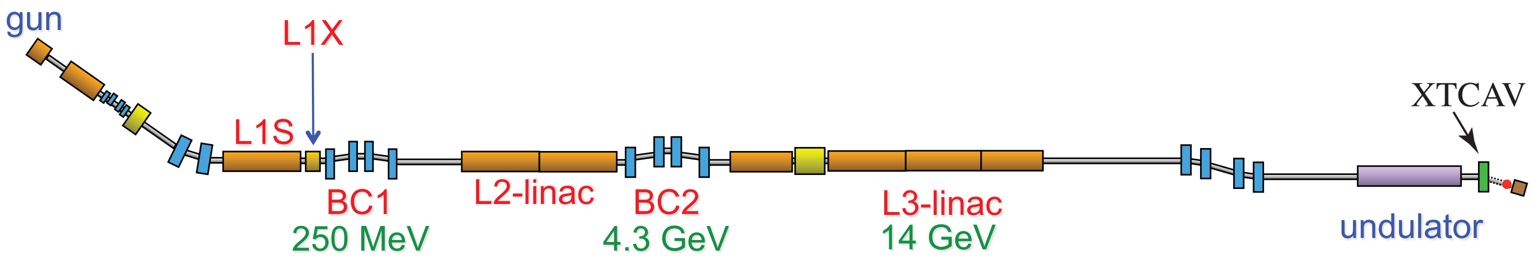

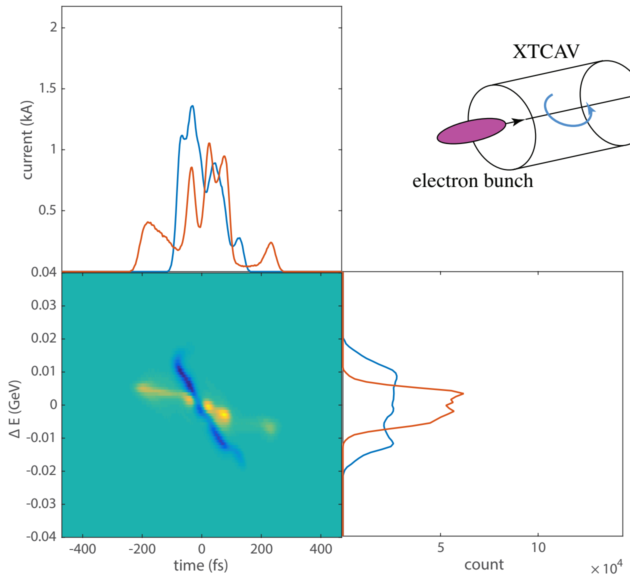

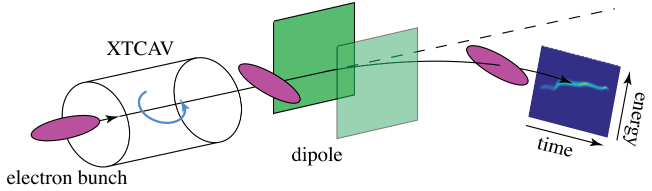

$$C = \int_{-\Delta L}^{\Delta L} \int_{-\Delta E}^{\Delta E} |\hat{\rho}(z,E) - \rho(z,E)|\, dEdz$$

TABLE I. Experiment setup details.

Experiment	Beam energy (GeV)	Bunch charge (nC)	k	α	ω	dt	Averaging	Cost function
1	4.48	0.17	1.0E-3	9	[2000, 2320, 2640, 2960, 3280, 3600]	8.7E-5	10×	1D projections
2	4.48	0.17	1.0E-3	4	[2000, 2320, 2640, 2960, 3280, 3600]	8.7E-5	10×	1D projections
3	13.42	0.18	1.4E-5	10	1000	6.3E-4	none	2D images

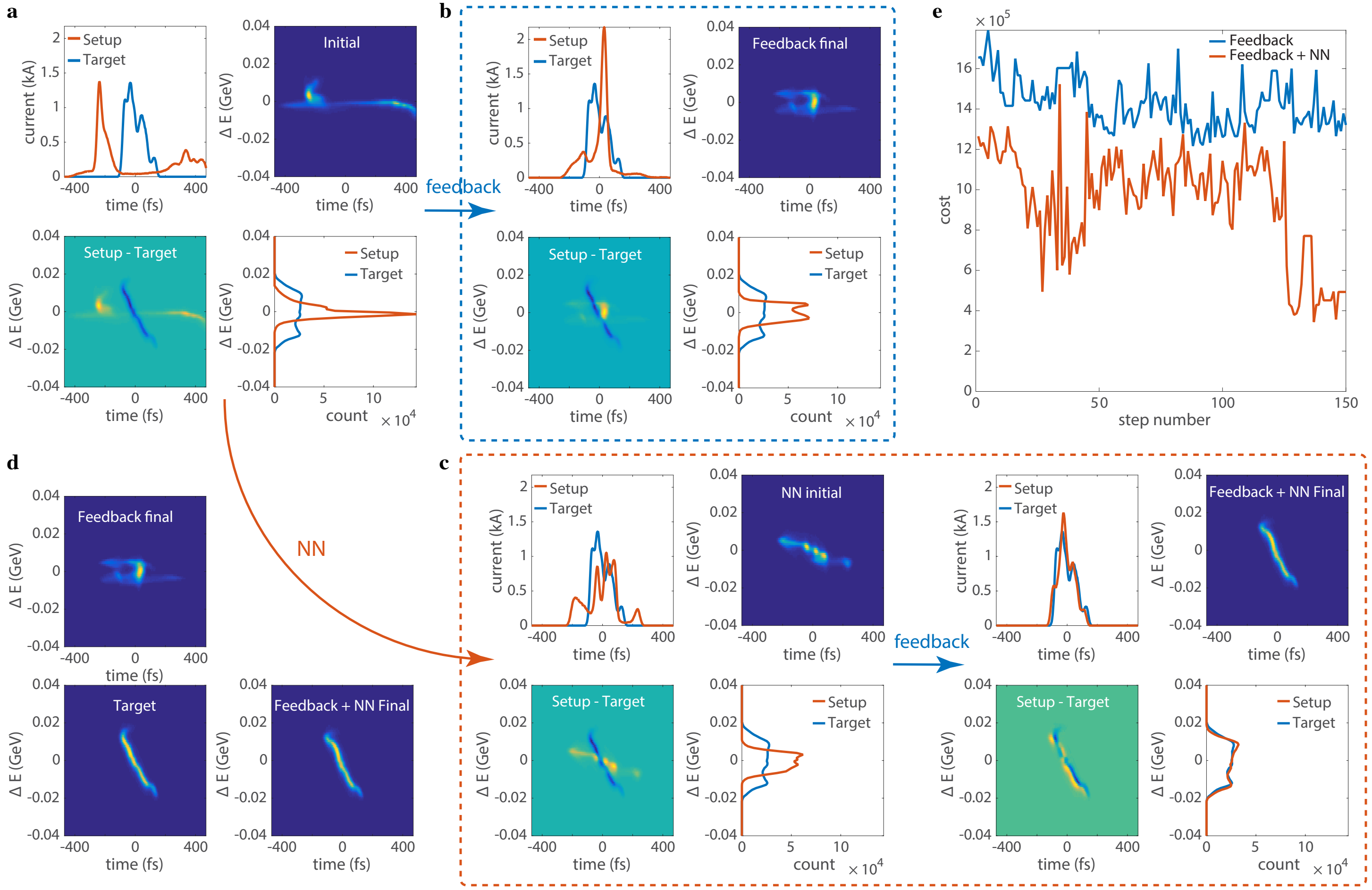
a
Setup
Target
current (kA)
time (fs)
Initial
Δ E (GeV)
Setup - Target
count
× 10^4
feedback
b
Feedback final
NN
c
NN initial
Feedback + NN Final
d
e
Feedback
Feedback + NN
× 10^5
cost
step number